

Disentangling the Seesaw in the Left-Right Model – An Algorithm for the General Case

JOSHUA KIERS^{1*}, KEN KIERS^{2†}, ALEJANDRO SZYNKMAN^{3‡}, TATIANA TARUTINA^{4§}

¹*Department of Mathematical and Computational Sciences, Marian University,
3200 Cold Spring Rd., Indianapolis, IN 46222, United States*

²*Physics Department, Taylor University,
1846 Main Street, Upland, Indiana 46989, United States*

³*IFLP, CONICET - Dpto. de Física, Universidad Nacional de La Plata,
C.C. 67, 1900 La Plata, Argentina*

⁴*IFLP, CONICET,
Diagonal 113 e/ 63 y 64, 1900 La Plata, Argentina*

Abstract

Senjanović and Tello have analyzed how one could determine the neutrino Dirac mass matrix in the minimal left-right model, assuming that the mass matrices for the light and heavy neutrinos could be taken as inputs. They have provided an analytical solution for the Dirac mass matrix in the case that the left-right symmetry is implemented via a generalized parity symmetry and that this symmetry remains unbroken in the Dirac Yukawa sector. We extend the work of Senjanović and Tello to the case in which the generalized parity symmetry is broken in the Dirac Yukawa sector. In this case the elegant method outlined by Senjanović and Tello breaks down and we need to adopt a numerical approach. Several iterative approaches are described; these are found to work in some cases but to be highly unstable in others. A stable, prescriptive numerical algorithm is described that works in all but a vanishingly small number of cases. We apply this algorithm to numerical data sets that are consistent with current experimental constraints on neutrino masses and mixings. We also provide some additional context and supporting explanations for the case in which the parity symmetry is unbroken.

*jkiers@marian.edu

†knkiers@taylor.edu

‡szynkman@fisica.unlp.edu.ar

§tarutina@fisica.unlp.edu.ar

1 Introduction

The observation of neutrino oscillations [1] proved that at least two neutrinos are massive particles. However, the origin of neutrino mass is still an open question; better understanding of this fundamental issue could yield key insights into the nature of physics beyond the Standard Model (SM). The seesaw mechanism is an appealing possibility that could account for the smallness of the neutrino mass scale [2–5]. There is not one unique seesaw model for neutrino mass, however, so even confirming that the seesaw mechanism is the source of neutrino mass does not necessarily lead to a complete understanding of the underlying model.

Seesaw models generically contain two types of Yukawa terms that couple the Higgs and lepton fields. The first is familiar from the SM and couples the left- and right-handed projections of the lepton fields. In the neutral sector, the resulting mass matrix is called the Dirac mass matrix and is denoted by M_D . The second couples the left-handed projections of the lepton fields to their charge-conjugates, and similarly for the right-handed fields, giving rise to so-called Majorana mass terms. In the seesaw mechanism, the mass matrix for the light neutrinos results from the interplay between these Dirac and Majorana mass terms.

As noted in Ref. [6], it is interesting to compare the situation for neutrinos to that for the charged fermions. In the Standard Model, the charged fermions receive their masses through their Yukawa interactions with the Higgs field. As a result, the measured values of their masses lead directly to predictions for the partial widths for Higgs decays into fermion-antifermion pairs. Measurements made at the Large Hadron Collider (LHC) have so far been compatible with the SM predictions [7]. The situation is considerably more complicated in the neutrino sector if the seesaw mechanism is at play. In this case, following the analogy from the charged fermions, one would want to determine the elements of the Dirac mass matrix M_D as a function of the light neutrino masses and mixings and those of the heavy states.¹ The former are being carefully investigated at current neutrino experiments and the latter could possibly be measured at the LHC or some future collider [6].

In the simplest formulation of the seesaw mechanism, the Dirac mass matrix M_D cannot be uniquely determined from the light and heavy mass matrices (M_ν and M_N , respectively), since it can always be redefined by an arbitrary complex orthogonal matrix [12, 13]. Within the context of the left-right symmetric extension of the SM [14–17], however, where the seesaw mechanism arises as a direct consequence of spontaneous left-right symmetry breaking, the matrix M_D is defined only in terms of physical quantities (see Refs. [6, 18–20]). At the level of the underlying model, left-right symmetry may be implemented by imposing a generalized charge conjugation symmetry, \mathcal{C} , or a generalized parity symmetry, \mathcal{P} . The charge conjugation approach has been analyzed in Ref. [18]; in this case it is argued that the relation between M_D and the masses and mixings of the light and heavy neutrino states is significantly simplified due to the fact that M_D is symmetric. As noted in Ref. [6], however, the generalized parity case is highly nontrivial and contains two distinct possibilities, depending on whether or not \mathcal{P} remains unbroken in the Dirac Yukawa sector. If \mathcal{P} is unbroken in the Dirac Yukawa sector, M_D is Hermitian² and may be determined analytically, given the masses and mixings of the light and heavy neutrino states [6, 20]. We shall refer to this as the “parity-conserving” scenario in the remainder of this work. By way of contrast, in the “parity-

¹A reverse path is adopted in Refs. [8–11] where the heavy neutrino mass matrix is determined from M_D and the light neutrino mass matrix.

²Actually, M_D is Hermitian up to multiplication by a diagonal sign matrix in this case. Please see below for further details.

violating” scenario M_D is no longer Hermitian³ and the analytical approach to determining M_D breaks down. Nevertheless, the authors of Ref. [6] develop a phenomenological analysis that would possibly allow one to determine M_D through the study of specific processes in this scenario. In summary, the left-right model, in which the parity-violating nature of the weak interactions follows from the spontaneous breaking of the left-right symmetry, turns out to be a theoretical picture that not only results in non-zero neutrino mass but also elucidates its origin.

In this article we develop a general method to determine M_D in the left-right model in the case that the underlying model (before spontaneous symmetry breaking) is invariant under \mathcal{P} . Our determination of M_D only relies on the knowledge of M_ν and M_N , as well as information related to the VEVs of the bidoublet Higgs field. In this way it is analogous to the analytical solution found in Refs. [6, 19, 20] for the parity-conserving limit, where M_D is obtained directly from these two matrices and the ratio of the bidoublet Higgs VEVs. What distinguishes our approach from previous work is that our approach does not assume that parity is conserved in the Dirac Yukawa sector after spontaneous symmetry breaking. That is, we assume that M_D could be non-Hermitian. In previous approaches, determination of M_D in the parity-violating case required the study of additional specific processes.⁴

To determine M_D from M_ν and M_N one needs to solve a system of non-linear matrix equations. The solution presented for the parity-conserving case in Refs. [6, 19, 20] is obtained through an ingenious procedure that makes use of the hermiticity of M_D . When parity is broken, M_D may no longer be assumed to be Hermitian and the procedure breaks down. In this case, the authors show that a solution can in principle be obtained numerically as an expansion in a small parameter, although they do not present a specific numerical algorithm to implement this strategy. A key feature of their proposed strategy in the parity-violating case is that the non-Hermitian matrix M_D is replaced by a Hermitian matrix that is a function of M_D . The method presented in the current work extends the approach outlined in Ref. [6] and provides a systematic prescription to solve for M_D numerically, even in the case that it is non-Hermitian. In a sense one could say that it adds a piece to the puzzle of unwinding the seesaw as the origin of neutrino mass. In the parity-conserving case, the analytical solution described in Refs. [6, 19, 20] allows one to resolve the seesaw by determining M_D in terms of M_ν and M_N . In the parity-violating case one could use the phenomenological approach outlined in Refs. [6, 19] to determine M_D . Of course, one could also apply that phenomenological analysis when parity is conserved, which would allow one to cross-check the values of M_D extracted from experiment with those corresponding to the analytical solution. Likewise, in the parity-violating case, the matrix M_D that would result from experiment could also be compared with the method proposed in this study, allowing one to further resolve the puzzle.

To illustrate our method and study its performance we undertake a numerical analysis using several theoretical data sets that are compatible with the current experimental constraints on the lepton masses and mixings. We use a Monte Carlo algorithm to generate these data sets, following the framework and approach described in Refs. [28, 29]. The Monte Carlo algorithm provides M_ν , M_N and M_D in each case, allowing us to take the matrices M_ν and M_N as inputs and to determine

³To be more precise, in this case the Vacuum Expectation Values (VEVs) of the bidoublet Higgs field contain a CP-violating phase that breaks the generalized parity symmetry in the Dirac Yukawa sector and leads to M_D no longer being Hermitian.

⁴As noted above, the method proposed in this paper requires the masses and mixings of the heavy neutrinos contained in M_N , therefore those processes [21–27] that would allow one to determine that information are still necessary.

whether our approach is able to recover the corresponding matrix M_D . Most of the data sets are of the parity-violating variety, but we also consider one parity-even data set so that we can test our method in this case as well. We find that our method successfully obtains a solution for M_D for all of the data sets that we study. Throughout this analysis we assume the normal ordering of neutrino masses⁵ and ignore the possibility of light sterile neutrinos.

Our paper is organized as follows. In Section 2 we outline the specific version of the Left-Right Model that we employ, including various details about our notation. Section 3 contains a detailed description of our method for determining M_D . This method is then illustrated with three numerical examples in Section 4. In Section 5 we briefly discuss alternative methods that we had previously used in our attempts to determine a solution for M_D . These approaches were successful for some of the data sets, but were unstable for others, illustrating the significant challenge posed by solving the set of nonlinear matrix equations to determine M_D . Section 6 contains a proof of a key mathematical relation used in Section 3, as well as derivations of several mathematical properties for the parity-conserving case considered in Refs. [6, 20]. We conclude with a brief discussion of our results in Section 7. Finally, the Appendices outline the diagonalization of the charged and neutral mass matrices, details of the notation and specifics about the method and also include some mathematical results related to the parameterization of complex orthogonal matrices.

2 The Model

In this section we provide a brief summary of the Left Right Model (LRM), primarily following the notation and conventions used in Ref. [28]; the interested reader is referred to Ref. [28] for more detail.

The underlying symmetry of the LRM is based on the gauge group $SU(2)_L \times SU(2)_R \times U(1)_{B-L}$. The specific formulation of the LRM considered in Ref. [28] contains two Higgs triplet fields,

$$\Delta_{L,R} = \begin{pmatrix} \delta_{L,R}^+/\sqrt{2} & \delta_{L,R}^{++} \\ \delta_{L,R}^0 & -\delta_{L,R}^+/\sqrt{2} \end{pmatrix}, \quad (1)$$

as well as a bidoublet Higgs field,

$$\phi = \begin{pmatrix} \phi_1^0 & \phi_1^+ \\ \phi_2^- & \phi_2^0 \end{pmatrix}. \quad (2)$$

The Yukawa terms for the charged and neutral leptons may then be written as [28]

$$-\mathcal{L}_{\text{Yukawa}} = \bar{\psi}'_{iL} \left(G_{ij} \phi + H_{ij} \tilde{\phi} \right) \psi'_{jR} + \frac{i}{2} F_{ij} \left(\psi'^T_{iL} C \tau_2 \Delta_L \psi'_{jL} + \psi'^T_{iR} C \tau_2 \Delta_R \psi'_{jR} \right) + \text{h.c.}, \quad (3)$$

where $C = i\gamma^2\gamma^0$ and $\tilde{\phi} = \tau_2\phi^*\tau_2$, and where $\psi'_{iL,R}$ represent the left- and right-handed lepton doublets in the gauge basis,

$$\psi'_{iL,R} = \begin{pmatrix} \nu'_{iL,R} \\ e'_{iL,R} \end{pmatrix}, \quad (4)$$

⁵This is an arbitrary choice; an inverted ordering could be considered as well.

where i is a generation index. The matrices G and H are taken to be Hermitian, while F may be assumed to be complex symmetric without loss of generality.⁶ The model also contains an extra left-right parity symmetry, \mathcal{P} [6, 28, 30], under which

$$\psi'_{iL} \leftrightarrow \psi'_{iR}, \quad \phi \leftrightarrow \phi^\dagger, \quad \Delta_L \leftrightarrow \Delta_R. \quad (5)$$

The neutral Higgs fields obtain VEVs upon spontaneous symmetry breaking; the Higgs VEVs may be parameterized as follows,⁷

$$\langle \phi \rangle = \begin{pmatrix} k_1/\sqrt{2} & 0 \\ 0 & -k_2 e^{-ia}/\sqrt{2} \end{pmatrix}, \quad \langle \Delta_L \rangle = \begin{pmatrix} 0 & 0 \\ v_L e^{i\theta_L}/\sqrt{2} & 0 \end{pmatrix}, \quad \langle \Delta_R \rangle = \begin{pmatrix} 0 & 0 \\ v_R/\sqrt{2} & 0 \end{pmatrix}, \quad (6)$$

where k_1 , k_2 , v_L and v_R are all taken to be real and positive. If the phase a is a multiple of π , then $\langle \phi \rangle$ respects the generalized parity symmetry even after spontaneous symmetry breaking; we refer to this as the “parity-conserving” case insofar as the Dirac Yukawa sector is concerned. Experimental constraints suggest $v_R \gg k_1, k_2 \gg v_L$; also, we have [32]

$$k_1^2 + k_2^2 \simeq \frac{4m_W^2}{g^2} \simeq (246.2 \text{ GeV})^2. \quad (7)$$

As noted in Ref. [28], it is natural to assume that the ratio k_2/k_1 is of order m_b/m_t .

The Yukawa terms in the Lagrangian lead to mass terms for the charged and neutral leptons when the neutral Higgs fields acquire VEVs. The mass matrix for the charged leptons in the gauge basis is given by Ref. [28]

$$M_\ell = \frac{1}{\sqrt{2}} (-Gk_2 e^{-ia} + Hk_1). \quad (8)$$

Recalling that G and H are Hermitian, we see that M_ℓ is Hermitian if the phase a is a multiple of π (i.e., in the so-called parity-conserving case).

The neutral lepton sector is more complicated than the charged lepton sector, since the Yukawa Lagrangian generically leads to Majorana mass terms in addition to the “ordinary” Dirac mass terms. For three lepton generations, the mass matrix is a 6×6 complex symmetric matrix,

$$\begin{pmatrix} M_{LL}^\dagger & M_{LR} \\ M_{LR}^T & M_{RR} \end{pmatrix}, \quad (9)$$

where

$$M_{LR} = \frac{1}{\sqrt{2}} (Gk_1 - Hk_2 e^{ia}) \quad (10)$$

is a 3×3 Dirac mass matrix and where

$$M_{LL} = \frac{1}{\sqrt{2}} F v_L e^{i\theta_L} \quad (11)$$

and

$$M_{RR} = \frac{1}{\sqrt{2}} F v_R, \quad (12)$$

⁶See the discussion in Ref. [28], as well as Refs. [30, 31].

⁷Reference [28] uses the phase $\alpha = \pi - a$; here we follow the notation of Ref. [6] for the phase.

Senjanović, et al (Ref. [6]) and present work		Kiers, et al (Ref. [28])
m_e (diagonal)	\leftrightarrow	M_ℓ
M_D	\leftrightarrow	M_{LR}^\dagger
M_N	\leftrightarrow	M_{RR}^*
M_ν	\leftrightarrow	$\left(M_{LL}^\dagger - M_{LR}M_{RR}^{-1}M_{LR}^T\right)^*$

Table 1: Correspondence between various mass matrices in Senjanović, et al (Ref. [6]) and those in Kiers, et al (Ref. [28]). Senjanović et al work primarily in a basis in which the charged lepton mass matrix is diagonal, whereas Kiers et al work in the gauge basis, in which neither the charged nor the neutral lepton mass matrices are assumed to be diagonal. The precise relations between the various matrices is given in Appendix A.

are 3×3 Majorana mass matrices for the left- and right-handed fields, respectively. As is evident from the above expressions, M_{LL} and M_{RR} are both complex symmetric matrices; M_{LR} is Hermitian if the phase a is a multiple of π . Equation (9) may be approximately block diagonalized (see Ref. [28] for details), which leads to 3×3 complex symmetric mass matrices for the (mostly) left- and (mostly) right-handed fields. The mass matrix for the right-handed neutrinos is simply M_{RR} , so that the right-handed neutrinos are generically quite heavy (due to the assumed large value of v_R). The mass matrix for the left-handed neutrinos is

$$M_{LL}^\dagger - M_{LR}M_{RR}^{-1}M_{LR}^T. \quad (13)$$

The first term is small, since it is proportional to v_L . The second term is suppressed due to the presence of M_{RR}^{-1} ; this suppression is known as the seesaw mechanism.

We have so far been working in the gauge basis. To make connections to measurable quantities, one needs to diagonalize the mass matrices for the charged and neutral leptons, which yields the physical lepton masses, as well as the Pontecorvo-Maki-Nakagawa-Sakata (PMNS) matrix. These quantities may then be measured or constrained by various types of experiments. The basis in which the mass matrices for the charged and neutral leptons are all diagonal is called the mass basis.

In the remainder of this paper we adopt the notation used by Senjanović et al in Ref. [6] and work in a basis that is part-way between the gauge basis and the mass basis [6]. In this basis, which we refer to as the “charged-diagonal” basis, one diagonalizes the mass matrix for the charged leptons and implements a corresponding transformation on the neutrino mass matrices. The neutrino mass matrices are not generally diagonal in this basis.

Table 1 shows the correspondence between the mass matrices in the charged-diagonal basis (of Senjanović et al) and those in the gauge basis (described above and in Ref. [28]). The table does not explicitly include the unitary matrices that are necessary to go from the gauge basis to the charged-diagonal basis. The interested reader is referred to Appendix A for the precise relations between quantities in these two bases.

It is straightforward to derive the following three relations between various mass matrices in the charged-diagonal basis,

$$M_D - U_e M_D^\dagger U_e = i s_a t_{2\beta} (e^{ia} t_\beta M_D + m_e), \quad (14)$$

$$U_e m_e U_e - m_e = i s_a t_{2\beta} (M_D + e^{-ia} t_\beta m_e), \quad (15)$$

$$M_\nu = \frac{v_L e^{i\theta_L}}{v_R} U_e^T M_N^* U_e - M_D^T \frac{1}{M_N} M_D, \quad (16)$$

where $\tan \beta \equiv k_2/k_1$ and where the unitary matrix U_e is associated with the transformation from the gauge basis to the charged-diagonal basis [see Eq. (77) in the Appendix for a precise definition]. Also, s_a , t_β and $t_{2\beta}$ stand for $\sin(a)$, $\tan \beta$ and $\tan(2\beta)$, respectively. Note that there is an overall sign ambiguity for U_e in the sense that Eqs. (14)-(16) are unchanged under $U_e \rightarrow -U_e$.

3 Description of Method

Our primary goal in this work is to describe a method that can be used to solve Eqs. (14), (15) and (16) for U_e and M_D , taking M_N , M_ν , $v_L e^{i\theta_L}/v_R$, a and β as inputs. The authors of Ref. [6] outlined such a procedure in the case that $s_a t_{2\beta} = 0$. In that case, Eqs. (14) and (15) reduce to the expressions $M_D = U_e M_D^\dagger U_e$ and $m_e = U_e m_e U_e$, respectively. Recalling that m_e is a real, diagonal matrix, we see that $U_e = \text{diag}(\pm 1, \pm 1, \pm 1)$ in this case, and that $M_D U_e^\dagger$ is Hermitian (we say that M_D is “sign Hermitian”). Armed with this knowledge, Senjanović et al were able to work out an analytical method to solve for M_D . They were also able to classify the solutions into various categories.

When $s_a t_{2\beta} \neq 0$, the analytical method devised in Ref. [6] breaks down, since M_D is no longer sign Hermitian. As we shall see, in this case it is possible to find a solution of Eqs. (14), (15) and (16) by using an iterative approach. We have applied this approach to various data sets and it appears to be quite stable (see Sec. 4 for further details).⁸

The starting point for our method is to define the matrix \mathcal{M} as in Ref. [6]:

$$\mathcal{M} = (M_D + e^{-ia} t_\beta m_e) U_e^\dagger. \quad (17)$$

The algorithm described below is designed to determine \mathcal{M} , which allows one to determine U_e (see Appendix B) and then finally to calculate M_D via

$$M_D = \mathcal{M} U_e - e^{-ia} t_\beta m_e. \quad (18)$$

A convenient property of \mathcal{M} is that it is Hermitian.⁹ Inspired by the mathematical manipulations that led to Eqs. (40) and (41) in Ref. [6], we substitute Eq. (18) into the complex conjugate of Eq. (16), multiply from the left by $\frac{1}{\sqrt{M_N}} U_e$ and from the right by $U_e^T \frac{1}{\sqrt{M_N}}$, and simplify, which yields

$$\begin{aligned} & \frac{v_L e^{-i\theta_L}}{v_R} I - \frac{1}{\sqrt{M_N}} U_e M_\nu^* U_e^T \frac{1}{\sqrt{M_N}} \\ &= \frac{1}{\sqrt{M_N}} (\mathcal{M} - e^{ia} t_\beta U_e m_e) \frac{1}{M_N^*} (\mathcal{M}^* - e^{ia} t_\beta m_e U_e^T) \frac{1}{\sqrt{M_N}}. \end{aligned} \quad (19)$$

We then define H , B and \tilde{H} as follows

$$H = \frac{1}{\sqrt{M_N}} \mathcal{M} \frac{1}{\sqrt{M_N^*}} \quad (20)$$

⁸We have also devised a number of other iterative approaches that are stable for some data sets, but not for others. These are described in Sec. 5.

⁹This follows from Eqs. (14) and (15).

$$B = e^{ia} t_\beta \frac{1}{\sqrt{M_N}} U_e m_e \frac{1}{\sqrt{M_N^*}}, \quad (21)$$

$$\tilde{H} = H - B, \quad (22)$$

so that

$$\tilde{H} \tilde{H}^T = (H - B)(H - B)^T = S, \quad (23)$$

where

$$S \equiv \frac{v_L e^{-i\theta_L}}{v_R} I - \frac{1}{\sqrt{M_N}} U_e M_\nu^* U_e^T \frac{1}{\sqrt{M_N}}. \quad (24)$$

Note that H is Hermitian, since \mathcal{M} is Hermitian and M_N is complex symmetric. Also, S is complex symmetric. The reader may note a certain amount of similarity between Eqs. (20)-(23) (above) and Eqs. (40) and (41) in Ref. [6]. A crucial difference, however, is that \tilde{H} is not generally Hermitian.

Since S is symmetric, we may write Eq. (23) in “symmetric normal form” as follows [33],

$$\tilde{H} \tilde{H}^T = S = O s O^T, \quad (25)$$

where O is a complex orthogonal matrix. In principle, the matrix s could be block diagonal; in practice, we assume that it is diagonal. Note that the elements in s are typically complex. As shown in Section 6, \tilde{H} itself can be written as

$$\tilde{H} = O \sqrt{s} \tilde{E} O^\dagger, \quad (26)$$

where \tilde{E} is a complex orthogonal matrix. Since H is Hermitian, we may write

$$H - H^\dagger = 0 = B - B^\dagger + O \sqrt{s} \tilde{E} O^\dagger - O \tilde{E}^\dagger \sqrt{s}^* O^\dagger, \quad (27)$$

which may be rearranged to give

$$\tilde{E} = \frac{1}{\sqrt{s}} O^T (B^\dagger - B) O^* + \frac{1}{\sqrt{s}} \tilde{E}^\dagger \sqrt{s}^*. \quad (28)$$

Denoting the j th element of the diagonal matrix \sqrt{s} by $\sqrt{|s_j|} e^{i\gamma_j}$, where γ_j is taken to be real, and defining

$$\Delta \tilde{B} \equiv \frac{1}{\sqrt{s}} O^T (B^\dagger - B) O^*, \quad (29)$$

we see that

$$\tilde{E}_{ij} = \Delta \tilde{B}_{ij} + \tilde{E}_{ji}^* \sqrt{\frac{|s_j|}{|s_i|}} e^{-i(\gamma_i + \gamma_j)}, \quad (30)$$

in which there is no implied sum over repeated indices. For future reference, we also define

$$\Delta_{ij} \equiv \tilde{E}_{ij} - \Delta \tilde{B}_{ij} - \tilde{E}_{ji}^* \sqrt{\frac{|s_j|}{|s_i|}} e^{-i(\gamma_i + \gamma_j)}. \quad (31)$$

According to Eq. (30), of course, this quantity should be zero for all i and j . Our numerical procedure seeks to determine values for the \tilde{E}_{ij} such that the Δ_{ij} are zero, or very close to zero. Once \tilde{E} is determined, one can eventually compute U_e and M_D .

3.1 Iterative procedure to solve for U_e and M_D

We now outline an iterative procedure that may be used to solve for U_e and M_D . Except for certain edge cases (to be described below), this procedure appears to be quite robust. A key to the success of this algorithm is the fact that, in practice, Eq. (24) is relatively well-approximated by making the replacement $U_e \rightarrow \tilde{I}$, where \tilde{I} is a diagonal matrix with ± 1 (as appropriate) down the diagonal.

In the description of the algorithm that follows, we denote quantities evaluated during the n -th iteration of the algorithm with an “ n ” subscript. In the first step of the n -th iteration of the algorithm, for example, we insert M_ν, M_N, a, β and $U_{e,n}$ into Eqs. (21) and (24) and use those expressions to calculate B_n and S_n . Our shorthand notation for this is as follows: “Eqs. (21) and (24): $M_\nu, M_N, a, \beta, U_{e,n} \rightarrow B_n, S_n$.” Adopting this shorthand throughout, we summarize the algorithm as follows,

1. Eqs. (21) and (24): $M_\nu, M_N, a, \beta, U_{e,n} \rightarrow B_n, S_n$.
2. Eq. (25): $S_n \rightarrow O_n, s_n$.
3. Eq. (29): $B_n, O_n, s_n \rightarrow \Delta \tilde{B}_n$.
4. Eq. (30): $\Delta \tilde{B}_n, s_n \rightarrow \tilde{E}_n$; if no solution is found for \tilde{E} , revise initial guess for U_e (denoted \tilde{I}) and/or the sign of the determinant of \tilde{E} , return to Step 1 and start over.
5. Eq. (26): $O_n, s_n, \tilde{E}_n \rightarrow \tilde{H}_n$.
6. Eq. (22): $\tilde{H}_n, B_n \rightarrow H_n$.
7. Eq. (20): $M_N, H_n \rightarrow \mathcal{M}_n$.
8. Eqs. (83)-(90) (and further discussion in Appendix B): $m_e, \tilde{I}, a, \beta, \mathcal{M}_n \rightarrow U_{e,n+1}$.
9. Eq. (18): $m_e, a, \beta, \mathcal{M}_n, U_{e,n+1} \rightarrow M_{D,n+1}$; return to Step 1.

We note the following:

- In the first step of the first iteration it is necessary to have a starting “guess” for U_e . Since $s_a t_{2\beta}$ is assumed to be small, a reasonable starting point is to choose one of the eight possibilities

$$\tilde{I} = \text{diag}(\pm 1, \pm 1, \pm 1). \quad (32)$$

- In Step 2 we use Eq. (25) to determine O_n and s_n . In practice, we compute the complex eigenvalues and eigenvectors of the complex, symmetric matrix S_n numerically (and assume that the eigenvalues are non-degenerate). Then we construct the complex matrix O_n and check that it is approximately orthogonal.
- Step 4 is the most challenging part of the algorithm. We have found in practice that if an incorrect set of signs has been chosen for \tilde{I} , it will not be possible to solve for \tilde{E}_n (hence the instruction at the end of Step 4).

- Once the correct \tilde{I} has been determined,¹⁰ it is typically sufficient to iterate through Steps 1-9 three to five times in order to determine U_e and M_D to within a reasonable amount of accuracy. We refer the reader to Sec. 4 for further details regarding the accuracy of the method.

3.2 Determination of \tilde{E}

The most challenging step in the algorithm described above is Step 4, in which we use Eq. (30) to solve for the elements of the complex orthogonal matrix \tilde{E} . In this subsection we describe how this may be accomplished. Throughout this subsection we suppress the index n that denotes the iteration number.

As we show in Appendix C, \tilde{E} can typically be parameterized as follows,¹¹

$$\tilde{E} = \begin{pmatrix} c_{\eta_1}c_{\eta_3} - c_{\eta_2}s_{\eta_1}s_{\eta_3}\xi & s_{\eta_1}s_{\eta_2} & c_{\eta_1}s_{\eta_3} + c_{\eta_2}c_{\eta_3}s_{\eta_1}\xi \\ s_{\eta_2}s_{\eta_3}\xi & c_{\eta_2} & -c_{\eta_3}s_{\eta_2}\xi \\ -c_{\eta_3}s_{\eta_1} - c_{\eta_1}c_{\eta_2}s_{\eta_3}\xi & c_{\eta_1}s_{\eta_2} & c_{\eta_1}c_{\eta_2}c_{\eta_3}\xi - s_{\eta_1}s_{\eta_3} \end{pmatrix}, \quad (33)$$

where $c_{\eta_i} \equiv \cos \eta_i$ and $s_{\eta_i} \equiv \sin \eta_i$ ($i = 1, 2, 3$), and where the angles η_1 , η_2 and η_3 are assumed to be complex. The parameter ξ is either $+1$ or -1 and is equal to the determinant of \tilde{E} . The goal in Step 4 is to determine three complex angles η_i and the sign of the discrete parameter ξ such that Eq. (30) is satisfied for all i and j . Parameterizing \tilde{E} as in Eq. (33) allows us to solve for the real and imaginary parts of the η_i in a relatively straightforward, prescriptive manner.

The real and imaginary parts of the 2-2 element of Equation (30) give the following two relations,

$$c_{\eta_2}^R = \Delta \tilde{B}_{22}^R + c_{\eta_2}^R \cos(2\gamma_2) - c_{\eta_2}^I \sin(2\gamma_2) \quad (34)$$

$$c_{\eta_2}^I = \Delta \tilde{B}_{22}^I - c_{\eta_2}^R \sin(2\gamma_2) - c_{\eta_2}^I \cos(2\gamma_2), \quad (35)$$

in which the R and I superscripts refer to the real and imaginary parts [e.g., $c_{\eta_2}^R \equiv \text{Re}(\cos(\eta_2))$]. Equations (34) and (35) are equivalent to each other, as may be seen by noting that $\sqrt{s}\Delta\tilde{B}$ is anti-Hermitian (see Eq. (29)). Rewriting Eq. (34) in terms of the real and imaginary parts of the complex angle η_2 yields the following expression,

$$\cosh(\eta_2^I) \cos(\eta_2^R) [1 - \cos(2\gamma_2)] = \Delta \tilde{B}_{22}^R + \sinh(\eta_2^I) \sin(\eta_2^R) \sin(2\gamma_2), \quad (36)$$

which has the two solutions

$$\eta_2^R = \alpha - \sin^{-1} \left(\frac{\Delta \tilde{B}_{22}^R}{\mathcal{G}} \right) \quad (37)$$

and

$$\eta_2^R = \alpha - \pi + \sin^{-1} \left(\frac{\Delta \tilde{B}_{22}^R}{\mathcal{G}} \right) \quad (38)$$

where

$$\alpha \equiv \tan^{-1} \left(\frac{(1 - \cos(2\gamma_2)) \cosh(\eta_2^I)}{\sinh(\eta_2^I) \sin(2\gamma_2)} \right) \quad (39)$$

¹⁰Recall that there is an overall sign ambiguity in U_e , so one actually expects two choices for \tilde{I} that yield solutions for M_D .

¹¹As explained in Appendix C, the parameterization in Eq. (33) does break down in certain edge cases (for example, when the 2-2 element of \tilde{E} is equal to unity). In most such cases, another angular parameterization could be used.

and

$$\mathcal{G} = \left[(1 - \cos(2\gamma_2))^2 \cosh^2(\eta_2^I) + \sinh^2(\eta_2^I) \sin^2(2\gamma_2) \right]^{\frac{1}{2}}, \quad (40)$$

as long as

$$\sinh^2(\eta_2^I) \geq \frac{(\Delta \tilde{B}_{22}^R)^2 - [1 - \cos(2\gamma_2)]^2}{2(1 - \cos(2\gamma_2))}. \quad (41)$$

The 1-2 and 2-1 elements of Equation (30) also give redundant relations, again due to the fact that $\sqrt{s}\Delta\tilde{B}$ is anti-Hermitian. The same may be said for the 2-3 and 3-2 elements. As a result, we are left with the following two complex relations,

$$s_{\eta_1} s_{\eta_2} = \Delta \tilde{B}_{12} + s_{\eta_2}^* s_{\eta_3}^* \xi \sqrt{\left| \frac{s_2}{s_1} \right|} e^{-i(\gamma_1 + \gamma_2)} \quad (42)$$

$$c_{\eta_1} s_{\eta_2} = \Delta \tilde{B}_{32} - s_{\eta_2}^* c_{\eta_3}^* \xi \sqrt{\left| \frac{s_2}{s_3} \right|} e^{-i(\gamma_2 + \gamma_3)}. \quad (43)$$

The above expressions allow us to express the complex quantities s_{η_1} and c_{η_1} as follows,

$$s_{\eta_1} = \mathcal{A} + \mathcal{B} s_{\eta_3}^*, \quad (44)$$

$$c_{\eta_1} = \mathcal{C} + \mathcal{D} c_{\eta_3}^*, \quad (45)$$

where $\mathcal{A}, \mathcal{B}, \mathcal{C}$ and \mathcal{D} are functions of s_{η_2} and $s_{\eta_2}^*$. Imposing the constraints $s_{\eta_1}^2 + c_{\eta_1}^2 = s_{\eta_3}^2 + c_{\eta_3}^2 = 1$, we have

$$1 = \mathcal{A}^2 + \mathcal{C}^2 + \mathcal{D}^2 + (\mathcal{B}^2 - \mathcal{D}^2) (s_{\eta_3}^*)^2 + 2\mathcal{A}\mathcal{B}s_{\eta_3}^* \pm 2\mathcal{C}\mathcal{D}\sqrt{1 - (s_{\eta_3}^*)^2}, \quad (46)$$

where $c_{\eta_3}^* \equiv \pm \sqrt{1 - (s_{\eta_3}^*)^2}$. Multiplying the two expressions in Eq. (46) by each other leads to a quartic equation in $s_{\eta_3}^*$, although in practice we typically solve the expressions in Eq. (46) as stated, since this seems to be more stable numerically.

To summarize, for a given value of η_2^I satisfying Eq. (41) there are two solutions for η_2^R (see Eqs. (37) and (38)). For both of these we may calculate $\eta_2 = \eta_2^R + i\eta_2^I$, and so compute s_{η_2} and then $\mathcal{A}, \mathcal{B}, \mathcal{C}$ and \mathcal{D} . For each value of η_2 we may solve Eq. (46) to obtain a total of four solutions for $s_{\eta_3}^*$ and the corresponding values of $c_{\eta_3}^*$. Back substitution into Eqs. (44) and (45) then yields s_{η_1} and c_{η_1} . Thus, for a given value of η_2^I satisfying Eq. (41) we generically expect a total of eight solutions for the sines and cosines of the complex angles η_1, η_2 and η_3 . It remains to ensure that the 1-1, 1-3 and 3-3 elements of Eq. (30) are satisfied. Recalling the definition for the quantity Δ_{ij} in Eq. (31), we define,

$$|\Delta|^2 \equiv |\Delta_{11}|^2 + |\Delta_{13}|^2 + |\Delta_{33}|^2, \quad (47)$$

which will generically have eight values for a given value of η_2^I . The goal of our algorithm is to find value(s) of η_2^I (and corresponding values for the various sines and cosines of the complex angles) that correspond to a zero (or, numerically, a minimum) of Eq. (47).

Then the method proceeds as follows:

4(a) Choose a value for ξ (either +1 or -1).

- 4(b) Choose a value for η_2^I . Compute the various combinations of sines and cosines of the complex angles η_1 , η_2 and η_3 that are consistent with the “central cross” elements of Eq. (30) [i.e., for $(i, j) = (1, 2), (2, 1), (2, 2), (2, 3)$ and $(3, 2)$], as described above.
- 4(c) Calculate $|\Delta|^2$ for the various combinations of sines and cosines of the complex angles identified in Step 4(b).
- 4(d) Repeat Steps 4(b) and 4(c), searching for combinations of the complex angles that yield $|\Delta|^2 \simeq 0$ (in practice, we use an algorithm that searches for a minimum of $|\Delta|^2$).
- 4(e) If no solutions are found that satisfy $|\Delta|^2 \simeq 0$, return to Step 4(a) and repeat the process for the opposite sign of ξ .

4 Numerical results

For our numerical analysis we implemented a Monte Carlo algorithm as described in Refs. [28, 29] to generate various data sets. The algorithm scans over random values of the Yukawa matrices defined in Eq. (3), searching for sets of parameters that are consistent with experimental constraints. For each set of Yukawa matrices, we were then able to compute m_e , M_ν , M_N , M_D , U_e and \tilde{E} . We generated, and subsequently analyzed, 16 data sets in this way; in each case, the neutrino masses and mixings satisfied the current experimental constraints at the 2σ level as given in Ref. [34].¹² In addition, we verified that the effective neutrino mass for neutrinoless double beta decay is always below the present limit [35]. For every data set we fixed $\tan\beta = k_2/k_1$ to 3/181 and $v_R = 50$ TeV [28].¹³ The remaining independent parameters, s_a and $|v_L|$, generally varied within ranges of $\mathcal{O}(10^{-2} - 1)$ and $\mathcal{O}(10^{-3} - 10^{-1})$ eV, respectively, whereas the phase of v_L took values between 0 and 2π . For one of the data sets we purposely set s_a to zero so that we could test our method on a parity-conserving data set. With these choices for the various parameters, the spectrum of the heavy neutrinos spanned from about 8 to 100 TeV. Our main focus in this section is not on performing a phenomenological analysis but on showing that the method described in Sec. 3 can be successfully applied to data sets that are consistent with experimental constraints, allowing us to recover the matrices U_e and M_D in each case. It is in this spirit that we are not particularly interested in a phenomenologically inspired spectrum for the heavy neutrinos.¹⁴

In the following subsections, we illustrate how the method described in Sec. 3 leads to solutions of Eqs. (14), (15) and (16) for three different scenarios.¹⁵ One of the three respects the generalized parity symmetry in the Dirac Yukawa sector after spontaneous symmetry breaking and the other two do not. Of the latter two, one has a relatively small value of $|s_a|$ (and is thus relatively “close” to the parity-conserving limit), while the other has a larger value of $|s_a|$. While we only consider

¹²The charged lepton masses generated by the routine typically agree with their corresponding experimental values to within a few parts in 10^4 .

¹³The authors of Ref. [28] introduce an extra $U(1)$ symmetry into the left-right model broken by a small dimensionless parameter ϵ . One of the advantages of this framework is that it allows scenarios consistent with neutrino phenomenology for a relatively low v_R scale. Since we followed this work, we also implemented the $U(1)$ horizontal symmetry in our analysis and fixed the value of ϵ to 0.3. Note that while the horizontal symmetry sets hierarchical scales for the Yukawa matrices, it does not impose relations among their elements. Therefore, the inclusion of this symmetry does not imply any loss of generality regarding the original problem of unwinding the seesaw.

¹⁴In any case, a lower heavy-neutrino spectrum could in principle be generated by decreasing the value of v_R .

¹⁵The computer code that implements the method is written in `Mathematica` and is available from the authors upon request.

these three data sets in detail, we emphasize that the method was successful for all 16 of the data sets. The calculation takes approximately 5 minutes for each dataset on a Desktop PC with Intel Core i7-9700K Processor (8x 3.60 GHz) and 16 GB RAM.

To study these three data sets we show plots of the quantity $|\Delta|^2$, defined in Eq. (47), as a function of $\text{Im}(\eta_2)$. Minimizing $|\Delta|^2$ is a key step in determining the elements of the matrix \tilde{E} , which then allows us to determine U_e and M_D . For each value of $\text{Im}(\eta_2)$ we determine the sines and cosines of the complex angles in the matrix \tilde{E} (see Eq. (33)) that are consistent with the “central cross” elements in Eq. (30). $|\Delta|^2$ is a measure of how well the remaining elements in this equation are satisfied; it is zero for solutions of Eq. (30). In principle, minima of $|\Delta|^2$ may need to be found several times, since the overall method is iterative. In the following, we show plots of $|\Delta|^2$ that are obtained after an appropriate number of iterations have been performed.

4.1 Parity conserving scenario

We first consider the parity conserving scenario ($s_a = 0$) that was noted above. For this example,

$$\tilde{E} = \begin{pmatrix} 0 & -1 & 0 \\ -1 & 0 & 0 \\ 0 & 0 & 1 \end{pmatrix}, \quad U_e = \begin{pmatrix} -1 & 0 & 0 \\ 0 & 1 & 0 \\ 0 & 0 & 1 \end{pmatrix}$$

and

$$M_D = \begin{pmatrix} 1.52 \times 10^{-5} & 3.21 \times 10^{-4} - 3.93 \times 10^{-5}i & -6.16 \times 10^{-4} + 1.97 \times 10^{-4}i \\ -3.21 \times 10^{-4} - 3.93 \times 10^{-5}i & 2.62 \times 10^{-3} & 1.93 \times 10^{-3} - 1.67 \times 10^{-3}i \\ 6.16 \times 10^{-4} + 1.97 \times 10^{-4}i & 1.93 \times 10^{-3} + 1.67 \times 10^{-3}i & 1.81 \times 10^{-3} \end{pmatrix}, \quad (48)$$

in which we have expressed M_D in units of GeV. The matrices \tilde{E} and U_e both have a form consistent with one of the expected forms for the parity-conserving case (see Section 6, as well as Ref. [6]). Also, aside from small numerical errors, $M_D U_e^\dagger$ is Hermitian, as is expected from Eq. (14).

Figure 1 shows a plot of $|\Delta|^2$ as a function of $\text{Im}(\eta_2)$.¹⁶ As is evident from the figure, the curves approach zero for $\text{Im}(\eta_2) \simeq 0$. We normally expect eight solutions for each value of $\text{Im}(\eta_2)$; to within numerical rounding errors, there are two sets of degenerate curves in this case (one set for each value of $\text{Re}(\eta_2)$ for a given value of $\text{Im}(\eta_2)$). We expect the degeneracies to be removed within parity-violating scenarios. In the following subsections we consider two data sets with $s_a \neq 0$. While both data sets illustrate the expected breaking of the degeneracy, one of them has $s_a \ll 1$ and exhibits some qualitative similarities to the parity-conserving scenario.

We note that since this data set has $s_a = 0$, we could also use the analytical solution method presented in Section III.A of Ref. [6] in this case. We have analyzed this data set using both the approach of Ref. [6] and the method described in the present work and have verified that they lead to consistent values of U_e and M_D , up to numerical rounding errors. Applying the method from Sec. 3 actually required some care in the parity-conserving scenario. Technically, in this scenario \mathcal{A} and \mathcal{C} are both zero in Eq. (46), so the equation for $s_{\eta_3}^*$ is quadratic. In practice we have found that small numerical errors lead to small but non-zero values for \mathcal{A} and \mathcal{C} . Attempting to solve Eq. (46) as a quartic equation in this case was not numerically stable, so we resorted to setting \mathcal{A} and \mathcal{C} to zero by hand and solving the resulting quadratic equation.

¹⁶As is noted in Sec. 6, our method assumes that $\tilde{E}_{22} \neq \pm 1$, a condition that is satisfied for this data set.

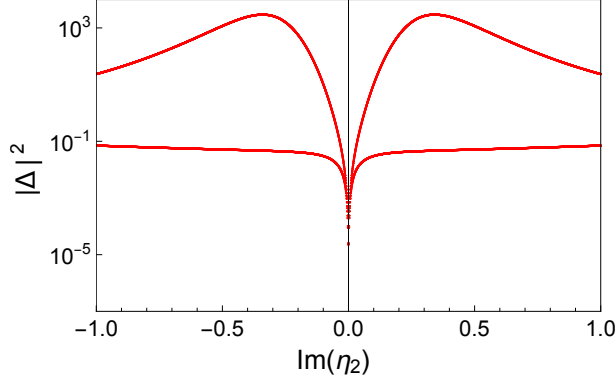


Figure 1: $|\Delta|^2$ vs. $\text{Im}(\eta_2)$ for the parity-conserving scenario.

Finally, we note that in the parity-conserving case, our routine also returns values for M_D that are different than the original one. When $s_a = 0$, it is clear from Eqs. (14)-(16) that $-M_D$ is also a solution; this is one of the new solutions that is returned. Interestingly, however, another solution emerges that has

$$\tilde{E} = \begin{pmatrix} 0 & 1 & 0 \\ 1 & 0 & 0 \\ 0 & 0 & 1 \end{pmatrix} \quad (49)$$

and, in units of GeV,

$$M_D = \begin{pmatrix} -2.63 \times 10^{-4} & -3.74 \times 10^{-4} - 2.64 \times 10^{-4}i & -2.28 \times 10^{-4} - 1.08 \times 10^{-4}i \\ 3.74 \times 10^{-4} - 2.64 \times 10^{-4}i & -2.24 \times 10^{-3} & -1.85 \times 10^{-3} + 6.18 \times 10^{-4}i \\ 2.28 \times 10^{-4} - 1.08 \times 10^{-4}i & -1.85 \times 10^{-3} - 6.18 \times 10^{-4}i & 1.10 \times 10^{-3} \end{pmatrix}, \quad (50)$$

in which we have dropped small numerical errors. The negative of the above expression for M_D is also returned. One can confirm by direct substitution that the new values for M_D are also solutions of Eqs. (14) and (16).

4.2 Parity-violating scenario I

We next consider a scenario with a small degree of parity violation ($s_a = 0.00187$). In this example,

$$\tilde{E} = \begin{pmatrix} -0.0159 - 0.0063i & 1.0000 + 0.0002i & -0.0134 + 0.0212i \\ 0.9999 - 0.0000i & 0.0160 + 0.0065i & -0.0056 + 0.0120i \\ 0.0052 - 0.0117i & 0.0136 - 0.0214i & 1.0002 + 0.0004i \end{pmatrix} \quad (51)$$

with

$$U_e = \begin{pmatrix} -1. + 8.09 \times 10^{-7}i & -5.20 \times 10^{-9} - 7.33 \times 10^{-8}i & 2.22 \times 10^{-9} + 6.69 \times 10^{-9}i \\ -5.20 \times 10^{-9} + 7.33 \times 10^{-8}i & 1. - 5.19 \times 10^{-7}i & 1.41 \times 10^{-8} + 1.02 \times 10^{-8}i \\ -2.22 \times 10^{-9} + 6.69 \times 10^{-9}i & 1.41 \times 10^{-8} - 1.02 \times 10^{-8}i & -1. + 5.33 \times 10^{-7}i \end{pmatrix} \quad (52)$$

and, in units of GeV,

$$M_D = \begin{pmatrix} -4.87 \times 10^{-6} + 1.58 \times 10^{-8}i & -1.25 \times 10^{-4} + 8.83 \times 10^{-6}i & -1.92 \times 10^{-4} + 6.38 \times 10^{-5}i \\ 1.25 \times 10^{-4} + 8.83 \times 10^{-6}i & -1.79 \times 10^{-5} + 3.27 \times 10^{-6}i & -2.76 \times 10^{-4} + 3.81 \times 10^{-4}i \\ -1.92 \times 10^{-4} - 6.38 \times 10^{-5}i & 2.76 \times 10^{-4} + 3.81 \times 10^{-4}i & -1.15 \times 10^{-3} + 5.50 \times 10^{-5}i \end{pmatrix}. \quad (53)$$

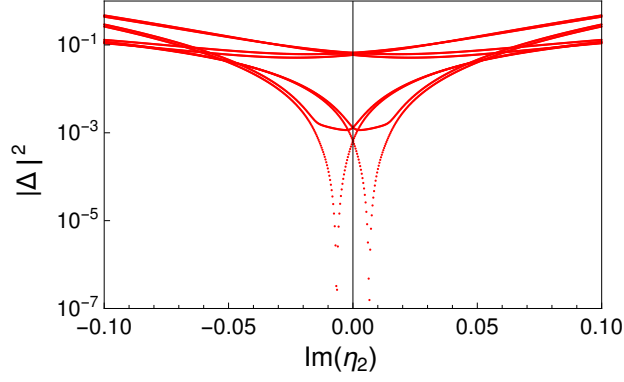


Figure 2: $|\Delta|^2$ vs. $\text{Im}(\eta_2)$ for parity-violating scenario I. Note that the horizontal and vertical scales are different than those of Figure 1.

Note that the matrix \tilde{E} in Eq. (51) has a relatively small value of \tilde{E}_{22} , whereas $\tilde{E}_{12} \approx \tilde{E}_{21} \approx \tilde{E}_{33} \approx 1$. All other elements of \tilde{E} are small compared to 1. Thus, as one might expect, \tilde{E} is “close” to one of the possible parity-conserving forms. Furthermore, M_D is quite close to being “sign-Hermitian” in this example, and U_e is close to being a diagonal sign matrix.

We applied our method to this data set and were able to determine the matrices M_D and U_e numerically. The results are numerically consistent with Eqs. (52) and (53). Figure 2 shows the corresponding 8-fold family of $|\Delta|^2$ versus $\text{Im}(\eta_2)$ curves. In this semilogarithmic plot, there are slower changing curves that correspond to larger values of $|\Delta|^2$ and curves that fall and rise abruptly in the solution region. It is seen that $|\Delta|^2$ approaches zero for $|\text{Im}(\eta_2)| \approx 0.0065$.

This case demonstrates several similarities to the one shown above in the parity-conserving scenario. The curves still have relatively low $|\Delta|^2$ values and two of them approach $|\Delta|^2 = 0$ at very small values of $\text{Im}(\eta_2)$. New features compared to the parity-conserving example are that the degeneracies in $|\Delta|^2$ have now been broken and that there are two values of $\text{Im}(\eta_2)$ (located symmetrically about zero) that yield solutions. These two values of $\text{Im}(\eta_2)$ yield the same solutions for M_D , ignoring small numerical errors. In practice we use the positive root.

4.3 Parity-violating scenario II

We now consider a scenario with a larger degree of parity violation ($s_a = -0.51$). For this example,

$$\tilde{E} = \begin{pmatrix} 3.467 + 2.494i & 2.623 - 0.525i & 1.881 - 3.866i \\ -0.350 + 0.427i & 1.052 + 0.148i & 0.036 - 0.162i \\ 2.540 - 3.346i & -0.465 - 2.628i & -3.973 - 1.831i \end{pmatrix} \quad (54)$$

with

$$U_e = \begin{pmatrix} 1. - 7.82 \times 10^{-4}i & 6.25 \times 10^{-7} + 6.63 \times 10^{-5}i & -9.87 \times 10^{-6} + 5.69 \times 10^{-7}i \\ 5.88 \times 10^{-7} - 6.63 \times 10^{-5}i & -1. - 2.25 \times 10^{-4}i & 2.74 \times 10^{-5} + 2.56 \times 10^{-5}i \\ -9.87 \times 10^{-6} - 5.64 \times 10^{-7}i & -2.74 \times 10^{-5} + 2.56 \times 10^{-5}i & -1. - 1.35 \times 10^{-4}i \end{pmatrix} \quad (55)$$

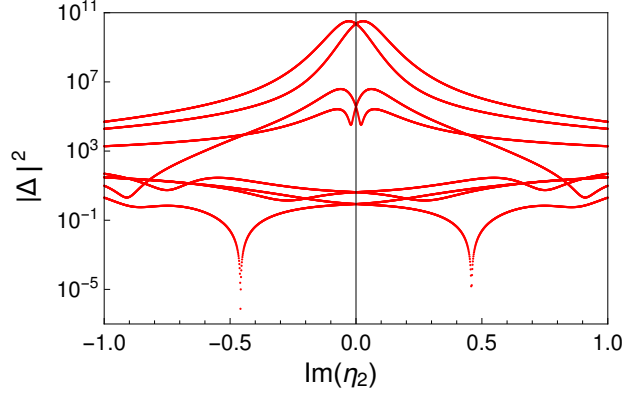


Figure 3: $|\Delta|^2$ vs. $\text{Im}(\eta_2)$ for parity-violating scenario II.

and, in units of GeV,

$$M_D = \begin{pmatrix} 5.45 \times 10^{-5} - 4.32 \times 10^{-6}i & 4.12 \times 10^{-4} - 3.76 \times 10^{-6}i & 5.95 \times 10^{-5} + 1.04 \times 10^{-3}i \\ -4.12 \times 10^{-4} - 3.78 \times 10^{-6}i & -1.31 \times 10^{-3} - 8.95 \times 10^{-4}i & 2.85 \times 10^{-3} - 3.05 \times 10^{-3}i \\ -5.94 \times 10^{-5} + 1.04 \times 10^{-3}i & 2.85 \times 10^{-3} + 3.05 \times 10^{-3}i & -3.09 \times 10^{-3} - 1.50 \times 10^{-2}i \end{pmatrix}. \quad (56)$$

The \tilde{E} matrix possesses larger values in this case and loses its resemblance to the \tilde{E} of the parity-conserving case. The matrices M_D and U_e are still relatively close to being sign-Hermitian and diagonal sign matrices, respectively, but they are not as close to those forms as were the corresponding expressions for the “almost” parity-conserving case (see Eqs. (53) and (52), respectively).

We were able to successfully apply our method to this example and recover values for U_e and M_D consistent with Eqs. (55) and (56). Figure 3 shows the corresponding $|\Delta|^2$ versus $\text{Im}(\eta_2)$ curves, with the solutions evident near $\text{Im}(\eta_2) \approx \pm 0.45$. In general, the curves reach significantly larger $|\Delta|^2$ values compared to the previous cases and their shapes noticeably differ from the curves of the parity-conserving scenario.

We have analyzed the convergence of the method for all of the parity-violating data sets and the conclusions are similar for all of them. As an illustration of that analysis we show the results obtained for the current scenario. Figure 4 shows two different measures of the relative error between the output of the method for U_e (M_D) and the true matrix U_e^0 (M_D^0) as a function of the number of iterations. These measures are defined as

$$\delta_l^{(1)} = \text{Max} \left(\sqrt{(\text{Re } a_l^{ij})^2 + (\text{Im } a_l^{ij})^2} \right), \quad \delta_l^{(2)} = \text{Max} \left(|\tilde{a}_l^{ij}|, |\tilde{b}_l^{ij}| \right) \quad (57)$$

for $i, j = 1, 2, 3$ and $l = U_e, M_D$, with

$$\begin{aligned} a_{U_e}^{ij} &= \frac{(U_e - U_e^0)^{ij}}{(U_e^0)^{ij}}, \quad a_{M_D}^{ij} = \frac{(M_D - M_D^0)^{ij}}{(M_D^0)^{ij}}, \\ \tilde{a}_{U_e}^{ij} &= \frac{\text{Re}(U_e - U_e^0)^{ij}}{\text{Re}(U_e^0)^{ij}}, \quad \tilde{b}_{U_e}^{ij} = \frac{\text{Im}(U_e - U_e^0)^{ij}}{\text{Im}(U_e^0)^{ij}}, \\ \tilde{a}_{M_D}^{ij} &= \frac{\text{Re}(M_D - M_D^0)^{ij}}{\text{Re}(M_D^0)^{ij}}, \quad \tilde{b}_{M_D}^{ij} = \frac{\text{Im}(M_D - M_D^0)^{ij}}{\text{Im}(M_D^0)^{ij}}. \end{aligned} \quad (58)$$

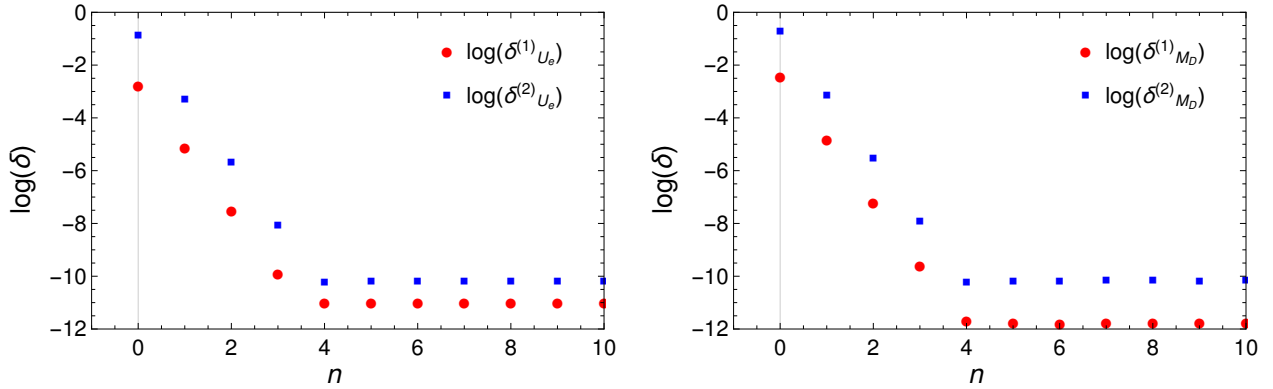


Figure 4: Convergence plot for U_e (left panel) and M_D (right panel) for parity-violating scenario II. Please see Eq. (57) for the definitions of $\delta_l^{(1)}$ and $\delta_l^{(2)}$, with $l = U_e, M_D$.

As can be seen from the figure, the convergence is extremely fast, precise and stable for both matrices.

5 Alternative Methods

In this section we describe some other numerical methods that we explored in our attempt to solve for U_e and M_D . It is worth noting from the beginning, however, that these alternative methods were not successful in finding solutions for all 15 of the parity-violating data sets. Only the method described in Section 3 (or slight variations on that method) was successful in this regard.

It is perhaps useful to restate the goal of our analysis. The equations that define the original problem are Eqs. (26), (27) and (31) in Ref. [6]; these are stated here as Eqs. (14), (15) and (16). Equations (14) and (15) come from the relations between M_D , m_e and the Yukawa matrices, and Eq. (16) is the seesaw formula for the light neutrino mass matrix. These equations constitute a system of coupled complex matrix equations for which we assume M_N and M_ν as experimental inputs and U_e and M_D as unknowns to be solved for.

In the following we briefly describe two alternative methods that implement different numerical approaches to solve U_e and M_D : A) a least squares minimization method and B) a fully iterative method.

5.1 Least squares minimization method

In our first attempt we employed a least squares minimization technique to solve the three coupled matrix equations (Eqs. (15) and (16), together with an equation expressing the unitarity condition for U_e ¹⁷). In this method the system of 3×3 complex matrix equations is transformed into a system of 51 equations for 36 unknown matrix elements. The quantity to minimize is the sum of

¹⁷If $s_a t_{2\beta} \neq 0$, Eqs. (14) and (15) are redundant. Since we are assuming the parity-violating case here, Eq. (14) can be removed from the system.

the squared differences between the left- and right-hand sides of those 51 equations when the solved values for the matrix elements of M_D and U_e are substituted. The least squares minimization was achieved employing a variant of the Newton method [36].

One complication in this approach is that the equations that we are attempting to solve have different dimensions – two of the matrix equations have dimensions of mass, while the third (expressing the unitarity of U_e) is dimensionless. Moreover, the order of magnitude of the matrix M_ν is 10^{-11} or 10^{-12} in units of GeV compared to 1 in the case of the unitarity condition. In view of this, we employed three normalization strategies: 1) no dimensional normalization was applied, but Eq. (16) was multiplied by a dimensionless numerical factor to compensate for the smallness of the matrix M_ν ; 2) the three equations of the system were transformed so that they have a unit matrix on their right-hand side; and 3) the three equations were transformed so that they have $m_e M_\nu m_e^{-2}$ on their right-hand side. We also considered a hybrid approach in which we first applied the third strategy and then used the output for U_e from that approach as a starting point when using the second strategy. This approach improved the accuracy in several cases. We analyzed these four strategies on the 15 data sets.

The least squares minimization approach to our problem attempts to minimize a particular sum of squares while traversing a 36-dimensional space of unknowns. This approach depends on the initial values chosen for the various unknowns. In our calculations we set the initial values for the matrix U_e to be $U_e = \text{diag}(\pm 1, \pm 1, \pm 1)$. These are reasonable starting points, since the actual U_e matrices for the parity-violating data sets are still somewhat well approximated by parity-conserving ones with a particular choice of signs. We found that this method does not converge when an incorrect combination of signs in $\text{diag}(\pm 1, \pm 1, \pm 1)$ is used. In general, we found that while it was possible to achieve a solution for all of the data sets using some of the above-mentioned strategies, none of these strategies worked for the entire collection of data sets. This illustrates the considerable difficulty in solving the problem at hand. By way of contrast, the method described in Sec. 3 does yield a solution for all of the data sets that we studied.

For the cases where the least squares minimization method leads to a solution, we compared the accuracy achieved to that achieved by the method in Sec. 3, using $\delta_{U_e}^{(1)}$ as a measure. The accuracy obtained by the method in Sec. 3 turns out to be two orders of magnitude higher on average. That method also ensures safer control over the solution search since it reduces the multi-dimensional space of unknown variables to lower dimensional regions at each stage of the procedure, whereas the least squares minimization method attempts to find all unknown variables at the same time.

5.2 Fully iterative method

Given the relatively low accuracy and the instability of the least squares minimization method described in the previous subsection, we have also investigated iterative approaches that are based on the analytical solution for the parity-conserving case (see Ref. [6]). In this subsection we describe various attempts along these lines. The goal of these approaches is to overcome the limitation imposed by the fact that M_D is not Hermitian when parity is violated.

We take as our starting point Eqs. (25) and (26). Noting that \tilde{H} can also be written as

$$\tilde{H} = \frac{1}{\sqrt{M_N}} U_e M_D^\dagger \frac{1}{\sqrt{M_N^*}}, \quad (59)$$

we find

$$U_e M_D^\dagger = \sqrt{M_N} O \sqrt{s} \tilde{E} O^\dagger \sqrt{M_N^*}, \quad (60)$$

from which it follows that

$$\tilde{E} = (\sqrt{M_N} O \sqrt{s})^{-1} U_e M_D^\dagger (O^\dagger \sqrt{M_N^*})^{-1}. \quad (61)$$

We also note that we may write a Riccati equation for U_e that derives from Eq. (15),

$$U_e m_e U_e = B_{\text{Riccati}}, \quad B_{\text{Riccati}} = i s_a t_{2\beta} (M_D + e^{-ia} t_\beta m_e) + m_e. \quad (62)$$

A solution of this equation is given by

$$U_e = \sqrt{B_{\text{Riccati}} m_e} m_e^{-1}, \quad (63)$$

where by the notation $\sqrt{B_{\text{Riccati}} m_e}$ we mean the principal root of the matrix $B_{\text{Riccati}} m_e$. Equation (62) actually has 8 solutions, which can be constructed by multiplying the principal root by diagonal matrices $\text{diag}(\pm 1, \pm 1, \pm 1)$.

The first algorithm that we designed consists of the following steps:

1. Set initial values for the matrices U_e and \tilde{E} (we take random complex matrices).
2. Use Eqs. (24) and (25) to calculate the orthogonal matrix O and diagonal matrix s .
3. Use Eq. (60) to calculate M_D using U_e and \tilde{E} set in Step 1, and O and s from Step 2.
4. Calculate U_e by solving Eq. (62) (we perform the calculation assuming 8 possibilities for the roots of the Riccati equation as indicated under Eq. (63)).
5. Use Eq. (61) to calculate \tilde{E} (after correcting O and \sqrt{s} with the updated U_e using Eqs. (24) and (25)), where the matrix $U_e M_D^\dagger$ is calculated from Eq. (14).
6. Orthogonalize \tilde{E} by iterating $\tilde{E} \rightarrow \frac{1}{2} (\tilde{E}^T + \tilde{E}^{-1})^T$ repeatedly.
7. Return to Step 2.

We can write this more succinctly using the shorthand notation adopted in Section 3:

1. Eq. (16): $U_{e_i}, \tilde{E}_i \rightarrow M_{D_i}$ (i stands for the i -th iteration)
2. Eq. (15): $M_{D_i} \rightarrow U_{e_{i+1}}$
3. Eq. (14): $M_{D_i}, U_{e_{i+1}} \rightarrow \tilde{E}_{i+1}$
4. Orthogonalize \tilde{E}_{i+1} ; back to Step 1

Unfortunately, this algorithm ended up being stable for only about the half of the 15 parity-violating data sets (in some cases we found that even when starting from the solution the algorithm diverges, leading to very distant regions in the parameter space). We also tried two different variations, setting instead the initial values for U_e and M_D as random complex matrices. These variations can be summarized as follows,

1. Eq. (16): $M_{D_i}, U_{e_i} \rightarrow \tilde{E}_i$
2. Orthogonalize \tilde{E}_i
3. Eq. (15): $M_{D_i} \rightarrow U_{e_{i+1}}$
4. Eq. (14): $\tilde{E}_i, U_{e_{i+1}} \rightarrow M_{D_{i+1}}$; back to Step 1

and

1. Eq. (16): $M_{D_i}, U_{e_i} \rightarrow \tilde{E}_i$
2. Orthogonalize \tilde{E}_i
3. Eq. (14): $\tilde{E}_i, U_{e_i} \rightarrow M_{D_{i+1}}$
4. Eq. (15): $M_{D_{i+1}} \rightarrow U_{e_{i+1}}$; back to Step 1

However, both variations led to results similar to those of the first algorithm, finding solutions for only about half of the data sets.

We also designed an alternative algorithm that did not use the Riccati equation. For this algorithm we only set the initial value for U_e as a random complex matrix. The algorithm proceeded as follows,

1. Eq. (15): $U_{e_i} \rightarrow M_{D_i}$
2. Eq. (14): $M_{D_i}, U_{e_i} \rightarrow \tilde{E}_i$
3. Orthogonalize \tilde{E}_i
4. Eq. (16): $M_{D_i}, \tilde{E}_i \rightarrow U_{e_{i+1}}$; back to Step 1

One might expect this algorithm to be more stable, since all four of the steps use the i -th iteration (instead of both the i -th and $(i+1)$ -th iterations at a given same step, as in the previous algorithms) and because it depends only on the initial value of U_e . However, this algorithm did not find a solution for any of the data sets.

Finally, we modified one of these algorithms using an approach inspired by the difference-map algorithm [37]. The difference-map algorithm is known to be able to find solutions to iterative mapping algorithms that are unstable. Unfortunately, while this approach seemed to show some promise, our attempts along these lines were also not successful for all of the data sets.

In summary, the fully iterative algorithms were not successful for all of the data sets. Our experience with these algorithms underscores the considerable difficulty of solving this system of complex, nonlinear matrix equations in order to unwind the seesaw mechanism in the parity-violating case. Fortunately, the prescriptive method described in Sec. 3 and illustrated in Sec. 4 does appear to be able to solve these equations, at least for all of the data sets considered.

6 Detailed analysis of the equation $HH^T = S$

In our efforts to extend the ideas of Ref. [20] to the parity-nonconserving case, we found it quite helpful to first understand the justification for every step in the analytical solution proposed in Ref. [20] for the parity-conserving case. It became clear to us how essential it is that H be Hermitian in order to derive an analytical solution. Yet, in case H is not Hermitian, it nonetheless proved beneficial to factor $H = O\sqrt{s}EO^\dagger$ and concentrate on solving for the entries of the complex orthogonal matrix E (which will no longer be a simple signed permutation matrix).

In this section, we thus provide additional context and supporting explanations for the analytical derivation carried out in Sec. III of Ref. [20]. Specifically, we will show how to derive the matrices in Eq. (37) of Ref. [20] under mild assumptions. We also discuss which of these assumptions are necessary and which can be removed.

The mathematical context is the following: we assume H is an unknown, Hermitian 3×3 matrix and that $S = HH^T$ is known. The goal is to solve for H given S . As in Eq. (27) of Ref. [20], we assume that $S = OsO^T$ has been placed in “symmetric normal form”; here O is a complex orthogonal matrix and s is block diagonal with symmetric Jordan blocks. Precise details can be found in Section XI.3 of Ref. [33]; we will only consider the case when s is diagonal for the sake of simplicity.

The central claim is that $H = O\sqrt{s}EO^\dagger$, where E is a signed permutation matrix whose form is determined by s . In fact, even in the parity-violating case (when H is not Hermitian), one can decompose H as $H = O\sqrt{s}EO^\dagger$ for some complex orthogonal matrix E , as the next lemma shows. Any further specification of E is precisely linked to the assumption that H is Hermitian.

Lemma 1. *Suppose that H is an invertible complex square matrix (not necessarily Hermitian), O is a complex orthogonal matrix, and s is a diagonal matrix such that $HH^T = OsO^T$. Then for any choice of square root \sqrt{s} , there exists a complex orthogonal matrix E such that $H = O\sqrt{s}EO^\dagger$.*

We begin by observing that

$$HH^T = O\sqrt{s}(O\sqrt{s})^T;$$

therefore

$$I = (H^{-1}O\sqrt{s})(H^{-1}O\sqrt{s})^T,$$

so $H^{-1}O\sqrt{s}$ is some complex orthogonal matrix, say P^{-1} . Rearranging, we have

$$\begin{aligned} H^{-1}O\sqrt{s} &= P^{-1} \\ O\sqrt{s}P &= H. \end{aligned}$$

Note that O^\dagger is a complex orthogonal matrix since O is. Thus if we define $E = P(O^{-1})^\dagger$, E is once again complex orthogonal and $P = EO^\dagger$. Thus $H = O\sqrt{s}EO^\dagger$ for a complex orthogonal matrix E .

In addition to the assumption that s is diagonal (which is made in Section III.D(i) of Ref. [20]), we further assume that

- (1) s has nonzero eigenvalues,

(2) s has distinct eigenvalues.

All of the above assumptions are mild in a probabilistic sense: they hold with probability 1 in the space of all possible matrices H . Later we will show that assumption (2) is necessary for the analytical solution described in Ref. [20], for otherwise one can exhibit infinitely many matrices H with $HH^T = S$. In contrast, we show that assumption (1) is not necessary.

6.1 Determination of E_I , E_{II}

The number of nonreal eigenvalues of s is even; moreover such eigenvalues come in complex conjugate pairs. As mentioned in Eq. (24) and following of Ref. [20], this is due to the characteristic polynomial of $S = HH^T$ having real coefficients whenever H is a Hermitian matrix.

Under the assumption that s is of size 3×3 , there are thus only two cases:

- (I) All eigenvalues are real: $s = \text{diag}(s_0, s_1, s_2)$, each $s_i \in \mathbb{R}$.
- (II) There is one pair of complex conjugate eigenvalues: $s = \text{diag}(z, s_0, z^*)$, $s_0 \in \mathbb{R}$.

In either case, one can find a diagonal matrix \sqrt{s} such that $\sqrt{s}\sqrt{s} = s$. Moreover, one may assume that the complex entries of \sqrt{s} come in conjugate pairs.

Proposition 1. *Assume that s is diagonal, satisfies (1) and (2), and has eigenvalues ordered as in (I) or (II) above. Then H must be equal to one of the matrices*

$$O\sqrt{s}EO^\dagger,$$

where E comes from the finite list of possibilities:

$$E = \begin{pmatrix} \pm 1 & 0 & 0 \\ 0 & \pm 1 & 0 \\ 0 & 0 & \pm 1 \end{pmatrix}$$

in case (I) and

$$E = \begin{pmatrix} 0 & 0 & \epsilon \\ 0 & \pm 1 & 0 \\ \epsilon & 0 & 0 \end{pmatrix}$$

in case (II), here $\epsilon = \pm 1$ and we are just emphasizing that the two corner entries must be equal.

By Lemma 1, we can write $H = O\sqrt{s}EO^\dagger$ for some complex orthogonal matrix E . Now we observe the following:

$$\begin{aligned} H &= O\sqrt{s}EO^\dagger \\ H^\dagger &= O(\sqrt{s}E)^\dagger O^\dagger; \end{aligned}$$

therefore H is Hermitian if and only if $\sqrt{s}E$ is. Since we assumed H was Hermitian, we get the following equations:

$$\sqrt{s}E = E^\dagger \sqrt{s}^*$$

$$\sqrt{s}E\sqrt{s}^{*-1} = E^\dagger$$

The last equation can be rewritten as

$$\sqrt{s}E\sqrt{s}^{*-1} = E^{*-1} \quad (64)$$

since $E^T = E^{-1}$. Conjugating Eq. (64) yields

$$\sqrt{s}^* E^* \sqrt{s}^{-1} = E^{-1},$$

and now taking the inverse of both sides we get

$$\sqrt{s}E^{*-1}\sqrt{s}^{*-1} = E. \quad (65)$$

Combining Eqs. (64) and (65), we have

$$sEs^{*-1} = \sqrt{s}(\sqrt{s}E\sqrt{s}^{*-1})\sqrt{s}^{*-1} = \sqrt{s}E^{*-1}\sqrt{s}^{*-1} = E.$$

Therefore E commutes with s , but up to a conjugation. But this can be remedied, for we know that s^* is a diagonal matrix whose entries are just a permutation of the diagonal entries of s . In other words, there exists a permutation matrix Q (possibly the identity matrix) such that $s^* = QsQ^{-1}$, which implies $s^{*-1} = Qs^{-1}Q^{-1}$ by taking the inverse of both sides. As with all permutation matrices, Q is (real) orthogonal: $Q^T = Q^{-1}$. Putting this all together, we have

$$\begin{aligned} sEQs^{-1}Q^{-1} &= E, \\ s(EQ)s^{-1} &= EQ, \end{aligned}$$

so the complex orthogonal matrix EQ commutes with s .

Since s has distinct eigenvalues, EQ must be diagonal. The only diagonal 3×3 complex orthogonal matrices A are the eight possibilities for

$$A = \begin{pmatrix} \pm 1 & 0 & 0 \\ 0 & \pm 1 & 0 \\ 0 & 0 & \pm 1 \end{pmatrix},$$

because of the requirement that $A^2 = AA^T = I$.

Finally, to establish the form of the matrix E , and thus find all solutions H , we just analyze what Q was in cases (I) and (II), respectively.

- (I) If $s = \text{diag}(s_0, s_1, s_2)$ with each $s_i \in \mathbb{R}$, then $s = s^*$ already, so $Q = I$. Therefore E itself must be one of the 8 possibilities

$$E = \begin{pmatrix} \pm 1 & 0 & 0 \\ 0 & \pm 1 & 0 \\ 0 & 0 & \pm 1 \end{pmatrix}.$$

Moreover, all of these possibilities are realizable – that is, $O\sqrt{s}EO^\dagger$ is Hermitian in each case¹⁸.

¹⁸Note that this relies on the entries of s being nonnegative. Indeed, one can show (through a somewhat technical case-by-case argument) that if s has at least one negative eigenvalue, then this eigenvalue is repeated, violating assumption (2).

(II) If $s = \text{diag}(z, s_0, z^*)$, then

$$Q = \begin{pmatrix} 0 & 0 & 1 \\ 0 & 1 & 0 \\ 1 & 0 & 0 \end{pmatrix},$$

so

$$E = \begin{pmatrix} 0 & 0 & \pm 1 \\ 0 & \pm 1 & 0 \\ \pm 1 & 0 & 0 \end{pmatrix}.$$

However, only half of these are valid possibilities yielding $O\sqrt{s}EO^\dagger$ Hermitian. Indeed, let us write

$$E = \begin{pmatrix} 0 & 0 & \epsilon_1 \\ 0 & \epsilon_2 & 0 \\ \epsilon_3 & 0 & 0 \end{pmatrix},$$

where each $\epsilon_i = \pm 1$. Then

$$\sqrt{s}E = \begin{pmatrix} 0 & 0 & \epsilon_1\sqrt{z} \\ 0 & \epsilon_2\sqrt{s_0} & 0 \\ \epsilon_3\sqrt{z^*} & 0 & 0 \end{pmatrix},$$

which is Hermitian if and only if $\epsilon_1 = \epsilon_3$. So E must take on the form

$$E = \begin{pmatrix} 0 & 0 & \epsilon \\ 0 & \pm 1 & 0 \\ \epsilon & 0 & 0 \end{pmatrix},$$

where $\epsilon = \pm 1$.

6.2 Distinct eigenvalues are necessary

We want to point out that the assumption (2) of Proposition 1 concerning distinct eigenvalues is necessary in order to find only finitely many solutions for H .

Proposition 2. *If s is a diagonal matrix of dimension at least 2 with a repeated eigenvalue, then the equation $HH^T = OsO^T$ has infinitely many solutions (given O, s) with Hermitian H .*

It suffices to consider only the equation $H_0H_0^T = s$ by performing the change of variables $H_0 = O^{-1}H(O^{-1})^\dagger$. Indeed, H_0 is Hermitian if and only if H is. Moreover, seeing as

$$\begin{aligned} H_0H_0^T &= O^{-1}H(O^{-1})^\dagger(O^{-1})^*H^T(O^{-1})^T \\ &= O^{-1}HH^T(O^{-1})^T, \end{aligned}$$

we find that $H_0H_0^T = s$ if and only if $HH^T = OsO^T$.

First suppose s has a repeated real eigenvalue s_0 ; up to permutations assume

$$s = \text{diag}(s_0, s_0, s_1, \dots)$$

(the later eigenvalues may be real or come in complex conjugate pairs). We already know we can find a Hermitian matrix H_1 such that $H_1 H_1^T = \text{diag}(s_1, \dots)$ (so H_1 has dimension 2 smaller). Therefore it suffices to show that there are infinitely many Hermitian 2×2 matrices A such that

$$\left(\begin{array}{c|c} A & 0 \\ \hline 0 & H_1 \end{array} \right)^T = s;$$

i.e., such that $AA^T = \begin{pmatrix} s_0 & 0 \\ 0 & s_0 \end{pmatrix}$.

Set

$$A = \begin{pmatrix} a & ib \\ -ib & a \end{pmatrix},$$

with both $a, b \in \mathbb{R}$. Then as long as $a^2 - b^2 = s_0$, A is such a solution. The equation $a^2 - b^2 = s_0$ has infinitely many solutions for a, b (graphically, the points on that hyperbola); for example, if s_0 is nonnegative, then $a = \pm\sqrt{s_0 + b^2}$ for any choice of b gives a distinct solution.

Second, suppose s has a repeated complex (not real) eigenvalue z . Up to permutations assume

$$s = \text{diag}(z, z, z^*, z^*, s_0, \dots).$$

Once again it suffices to find infinitely many Hermitian matrices A such that $AA^T = \text{diag}(z, z, z^*, z^*)$.

Set

$$A = \begin{pmatrix} 0 & 0 & x & y \\ 0 & 0 & -y & x \\ \bar{x} & -\bar{y} & 0 & 0 \\ \bar{y} & \bar{x} & 0 & 0 \end{pmatrix}.$$

A straightforward calculation reveals that, as long as $x^2 + y^2 = z$, $AA^T = \text{diag}(z, z, z^*, z^*)$. Again there are infinitely many solutions to the equation $x^2 + y^2 = z$ (pick any $x \in \mathbb{C}$ and there is at least one solution for y).

6.3 Handling an unrepeated eigenvalue 0

Suppose $HH^T = OsO^T$ as before with s diagonal and having distinct eigenvalues (assumption (2)). Now suppose that s has 0 as one of its eigenvalues. Without loss of generality, we assume that $HH^T = s$ (using a change-of-basis as before) and that $s = \text{diag}(a, b, 0)$, where $a \neq 0, b \neq 0$.

Proposition 3. *Under the above assumptions, H must be of the form*

$$\left(\begin{array}{c|c} \bar{H} & 0 \\ \hline 0 & 0 \end{array} \right).$$

Let e_3 denote the standard column vector $\begin{pmatrix} 0 \\ 0 \\ 1 \end{pmatrix}$.

Note that the nullspace of s^* is spanned by e_3 . Set $v = H^T e_3$. Then $Hv = 0$ since $se_3 = 0$, so $H^T Hv = 0$ as well. Recalling that $s^* = H^*H = H^T H$, we see that $s^*v = 0$. Thus $v = ce_3$ for some scalar c . Now observe that

$$H^*e_3 = ce_3$$

$$He_3 = c^* e_3. \quad (66)$$

Since $0 = H(ce_3) = |c|^2 e_3$, we must have $c = 0$. Eq. (66) together with $c = 0$ implies that H is a Hermitian matrix whose last column is all 0's. In other words,

$$H = \left(\begin{array}{c|c} \bar{H} & 0 \\ \hline 0 & 0 \end{array} \right)$$

for some Hermitian 2×2 matrix \bar{H} .

Therefore the problem of solving for H reduces to solving for \bar{H} , and the smaller system

$$\bar{H}\bar{H}^T = \text{diag}(a, b)$$

can be solved as before.

7 Discussion and Conclusions

It is well known that at least two neutrinos are light massive particles. However, it remains crucial to understand the origin of neutrino mass. The seesaw mechanism is a compelling possibility but it needs to be probed as a consistent explanation. For the charged fermions, experiments support the SM explanation that ties the particles' masses to the corresponding Yukawa terms in the underlying theory. In the case of neutrinos, one would want to be able to determine the Dirac mass (M_D) between the left-handed neutrinos and the new neutral lepton singlets (N) in terms of the light neutrino masses and mixings (M_ν) and the mass matrix of the heavy states (M_N). Therefore, probing the seesaw requires the measurement of these two matrices and a scheme that allows the determination of M_D from them.

Within the context of minimal extensions of the SM, M_D is not unambiguously determined in terms of M_ν and M_N . This problem can be overcome, however, by including more structure in the theory. This is precisely the case for the left-right symmetric model, where the seesaw is a natural outcome of spontaneous symmetry breaking. In this paper we have studied the scenario in which the left-right symmetry is implemented via a discrete generalized parity, \mathcal{P} . In this scenario one can solve for M_D analytically using the approach described in Refs. [6, 20] as long as the bidoublet Higgs field has a real vacuum expectation value. In contrast, for a complex VEV, which induces \mathcal{P} parity violation in the Dirac Yukawa sector, the problem is more difficult to handle and an analytical solution is lacking. Although this case can in principle be addressed numerically, we are not aware of any defined numerical procedure in the literature. With the intention of filling this gap, the goal of this paper has been to design and test a prescriptive numerical method that allows one to determine M_D only from the physical information contained in the matrices M_ν and M_N .

For the parity-violating case, we have found that the problem of determining M_D is inherently tied to the knowledge of U_e , the unitary matrix associated with the transformation from the gauge basis to the charged-diagonal basis. Therefore, both matrices need to be solved simultaneously. The method proposed in this paper, as described in Sec. 3, fulfills this goal through an iterative procedure that has proven to be stable and has led to solutions for all of the tested data sets. We illustrated the procedure explicitly in Sec. 4 for three different data sets that had varying degrees of parity violation.

Finally, it is worth stressing the difficulty of the problem faced in this article. As a matter of fact, in Sec. 5 we presented alternative iterative methods that were stable for some data sets while not for others. The problem of probing the seesaw mechanism when parity is violated is important and challenging enough to require a robust solution method.

Acknowledgements

The authors wish to thank G. Senjanović for helpful communication and M. Assis and D. Simons for permission to use their computer code. The authors also thank T. Lehrian and W. Slauson for technical assistance. K.K. thanks Taylor University for financial support and for support during his sabbatical. T.T. and A.S. thank CONICET and ANPCyT (under projects PICT 2017-2751 and PICT 2018-03682).

A Connection to Notation in Ref. [28]

In this appendix we outline the procedure for diagonalizing the charged and neutral mass matrices and we also specify the relations between the charged-diagonal basis (used in Ref. [6] and in the present work) and the gauge basis (used in Ref. [28] and summarized at the beginning of Sec. 2).

Equations (8), (10), (11), (12) and (13) give the explicit expressions for M_ℓ , M_{LR} , M_{LL} , M_{RR} and the light neutrino mass matrix, respectively, in terms of Yukawa coupling matrices in the gauge basis. The charged lepton mass matrix may be diagonalized using a biunitary transformation as follows,

$$m_e \equiv M_\ell^{\text{diag}} = V_L^{\ell\dagger} M_\ell V_R^\ell, \quad (67)$$

where the elements of m_e are taken to be real and positive. The light and heavy neutrino mass matrices may also be diagonalized using unitary matrices,

$$M_\nu^{\text{diag}} = V_L^{\nu\dagger} \left(M_{LL}^\dagger - M_{LR} M_{RR}^{-1} M_{LR}^T \right) V_L^{\nu*}, \quad (68)$$

$$M_R^{\text{diag}} = V_R^{\nu T} M_{RR} V_R^\nu. \quad (69)$$

The unitary matrices used to diagonalize the charged and neutral lepton mass matrices are then used to construct the left- and right-handed PMNS matrices,

$$V_L = B_\phi^\dagger V_L^{\ell\dagger} V_L^\nu S_L, \quad (70)$$

$$V_R = B_\phi^\dagger V_R^{\ell\dagger} V_R^\nu S_R, \quad (71)$$

where B_ϕ is a diagonal phase matrix and S_L and S_R are diagonal sign matrices; these diagonal matrices are used to bring V_L and V_R into their conventional forms. Defining $\nu_{L,R}$ and $e_{L,R}$ to be the neutral and charged lepton fields in the mass basis (i.e., in the basis in which the mass matrices are diagonal), we have

$$\nu_{L,R} = S_{L,R}^\dagger V_{L,R}^{\nu\dagger} \nu'_{L,R}, \quad (72)$$

$$e_{L,R} = B_\phi^\dagger V_{L,R}^{\ell\dagger} e'_{L,R}, \quad (73)$$

where $\nu'_{L,R}$ and $e'_{L,R}$ are the corresponding fields in the gauge basis. The left- and right-handed PMNS matrices appear in the charged-current Lagrangian when it is written in terms of the fields in the mass basis,

$$\mathcal{L}_{CC} \simeq -\frac{g}{\sqrt{2}}\bar{e}_L V_L \gamma_\mu \nu_L W_L^{\mu-} - \frac{g}{\sqrt{2}}\bar{e}_R V_R \gamma_\mu \nu_R W_R^{\mu-} + \text{h.c.} \quad (74)$$

Finally, we note that the left-handed PMNS matrix is parameterized as follows in Ref. [31] (and in Ref. [28]),

$$V_L = \mathcal{U}^{(0)}(\theta_{12}, \theta_{23}, \theta_{13}, \delta_L) A_L, \quad (75)$$

where A_L is a diagonal matrix that may be written in terms of two Majorana phases, $A_L = \text{diag}(e^{i\alpha_1/2}, e^{i\alpha_2/2}, 1)$. The matrix $\mathcal{U}^{(0)}$ may be written as

$$\begin{aligned} & \mathcal{U}^{(0)}(\theta_{12}, \theta_{23}, \theta_{13}, \delta_L) \\ &= \begin{pmatrix} c_{12}c_{13} & s_{12}c_{13} & s_{13}e^{-i\delta_L} \\ -s_{12}c_{23} - c_{12}s_{23}s_{13}e^{i\delta_L} & c_{12}c_{23} - s_{12}s_{23}s_{13}e^{i\delta_L} & s_{23}c_{13} \\ s_{12}s_{23} - c_{12}c_{23}s_{13}e^{i\delta_L} & -c_{12}s_{23} - s_{12}c_{23}s_{13}e^{i\delta_L} & c_{23}c_{13} \end{pmatrix}, \end{aligned} \quad (76)$$

where s_{ij} and c_{ij} refer to the sines and cosines, respectively, of the (real) angles θ_{12} , θ_{13} and θ_{23} . The interested reader is referred to Ref. [28] for a parameterization of V_R .

Reference [6] works in a basis in which the charged lepton mass matrix is diagonal, but the neutrino mass matrices are not; we have called this basis the “charged-diagonal” basis. The diagonalization of the charged lepton mass matrix was shown above, in Eq. (67). Equations (14)-(16) also include the matrix U_e ; this matrix is defined in terms of the matrices V_L^ℓ and V_R^ℓ that are used to diagonalize M_ℓ ,

$$U_e = B_\phi^\dagger V_R^{\ell\dagger} V_L^\ell B_\phi. \quad (77)$$

It is straightforward to work out the relations between M_ν , M_N and M_D (which are defined in the charged-diagonal basis) and $M_{LL}^\dagger - M_{LR}M_{RR}^{-1}M_{LR}^T$, M_{RR} and M_{LR} (which are defined in the gauge basis). The specific relations are as follows,

$$M_\nu = B_\phi \left(V_L^\ell \right)^T \left(M_{LL}^\dagger - M_{LR}M_{RR}^{-1}M_{LR}^T \right)^* V_L^\ell B_\phi, \quad (78)$$

$$M_N = B_\phi^\dagger V_R^{\ell\dagger} M_{RR}^* V_R^{\ell*} B_\phi^\dagger, \quad (79)$$

$$M_D = B_\phi^\dagger V_R^{\ell\dagger} M_{LR}^\dagger V_L^\ell B_\phi. \quad (80)$$

B Numerical Determination of U_e for a Given \mathcal{M}

In this appendix we describe a procedure that can be used to determine U_e with a high degree of accuracy once an approximate expression for \mathcal{M} has been determined in Step 7 of the procedure described in Sec. 3.1; the procedure described here is used in Step 8 in that section. Our approach assumes that $s_a t_{2\beta}$ is somewhat small, in which case U_e is close to diagonal.¹⁹ One potential point

¹⁹The authors of Ref. [6] outlined an alternative approach for estimating U_e , which is to express it in terms of a series expansion in powers of $s_a t_{2\beta}$.

of confusion is that the method described in this Appendix is an iterative one that is itself used in the context of another iterative procedure (i.e., the one described in Sec. 3.1). In this Appendix we will suppress the index for the “Step #” in the larger iterative process. The index m that is used here refers to the m th step in the iterative process used to determine U_e for a given (i.e., fixed) step of the procedure described in Sec. 3.1.

We start by recalling the definition of \mathcal{M} in Eq. (17), which allows us to reexpress Eq. (15) as follows,

$$U_e m_e - m_e U_e^\dagger = i s_a t_{2\beta} \mathcal{M}, \quad (81)$$

where m_e is a diagonal matrix containing the charged lepton masses. In the limit that $s_a t_{2\beta}$ goes to zero, the unitary matrix U_e becomes a diagonal matrix whose non-zero entries are ± 1 . With this in mind, we define the matrix $U_e^{(m)}$ in terms of a product of $m + 1$ unitary matrices $U^{(j)}$,

$$U_e^{(m)} = \prod_{j=0}^m U^{(j)} = U^{(m)} U^{(m-1)} \dots U^{(1)} U^{(0)}, \quad (82)$$

where $U^{(0)} = \tilde{I}$ is the diagonal sign matrix defined in Eq. (32). The matrix U_e is taken to be the limit of Eq. (82) as m approaches infinity,

$$U_e = \lim_{m \rightarrow \infty} U_e^{(m)} = \prod_{j=0}^{\infty} U^{(j)}. \quad (83)$$

Each of the unitary matrices $U^{(j)}$ may be expressed as follows,

$$U^{(j)} = \exp\left(\sum_{i=1}^9 \frac{i\alpha_i^{(j)}}{2} \lambda_i\right) = 1 + \left(\sum_{i=1}^9 \frac{i\alpha_i^{(j)}}{2} \lambda_i\right) + \frac{1}{2!} \left(\sum_{i=1}^9 \frac{i\alpha_i^{(j)}}{2} \lambda_i\right)^2 + \dots, \quad (84)$$

where λ_i , $i = 1, \dots, 8$, are the usual Gell-Mann matrices, λ_9 is the unit matrix, and the $\alpha_i^{(j)}$ are real parameters that are to be determined.²⁰ The idea of the procedure is to determine matrices $U^{(1)}$, $U^{(2)}$, $U^{(3)}$, \dots , in such a way that $U^{(m)}$ approaches the identity matrix for large m (i.e., in such a way that the $\alpha_i^{(m)}$ approach zero for large m). This allows one to truncate the infinite product in Eq. (83), so that $U_e^{(m_{\max})}$ (for some m_{\max}) is used as a suitable approximation to U_e .

In the first step of the procedure we substitute

$$U_e^{(1)} = U^{(1)} \tilde{I} \quad (85)$$

into Eq. (81), in place of U_e , and then expand the expression for $U^{(1)}$ (see Eq. (84)) to linear order in the $\alpha_i^{(1)}$. This gives us the defining expression for the nine unknowns $\alpha_i^{(1)}$,

$$\left(1 + \sum_{i=1}^9 \frac{i\alpha_i^{(1)}}{2} \lambda_i\right) \tilde{I} m_e - m_e \tilde{I} \left(1 - \sum_{i=1}^9 \frac{i\alpha_i^{(1)}}{2} \lambda_i\right) = i s_a t_{2\beta} \mathcal{M}. \quad (86)$$

Defining $\tilde{m}_e^{(0)} \equiv \tilde{I} m_e$ and rearranging, we have

$$\sum_{i=1}^9 \frac{i\alpha_i^{(1)}}{2} \left(\lambda_i \tilde{m}_e^{(0)} + \tilde{m}_e^{(0)\dagger} \lambda_i\right) = i s_a t_{2\beta} \mathcal{M} - \tilde{m}_e^{(0)} + \tilde{m}_e^{(0)\dagger}. \quad (87)$$

²⁰Note that we cannot assume that the $U^{(j)}$ are special unitary, which is why we need to include a ninth matrix in our basis.

To solve for the $\alpha_i^{(1)}$, we multiply the above expression by λ_k and take the trace,

$$\sum_{i=1}^9 \frac{i\alpha_i^{(1)}}{2} \text{Tr} \left[\left(\lambda_i \tilde{m}_e^{(0)} + \tilde{m}_e^{(0)\dagger} \lambda_i \right) \lambda_k \right] = \text{Tr} \left[\left(i s_a t_{2\beta} \mathcal{M} - \tilde{m}_e^{(0)} + \tilde{m}_e^{(0)\dagger} \right) \lambda_k \right], \quad (88)$$

which yields nine equations (for $k = 1, 2, \dots, 9$) in the nine unknowns. Once we have determined the $\alpha_i^{(1)}$, we use the series expansion of Eq. (84) to determine the matrix $U^{(1)}$ (summing up enough terms so that the result is very close to unitary). While the linearized version of $U^{(1)}$ was an exact solution of Eq. (86), the “re-unitarized” version of the matrix (i.e., $U^{(1)}$) is no longer a solution when Eq. (85) is substituted into Eq. (81). This brings us to the next step in the procedure.

In the second step we substitute

$$U_e^{(2)} = U^{(2)} U^{(1)} \tilde{I}, \quad (89)$$

into Eq. (81) and expand $U^{(2)}$ to linear order in the coefficients $\alpha_i^{(2)}$, while keeping the matrix $U^{(1)}$ in its exactly unitary form. Performing the same manipulations as in the previous step, we obtain the following expression for the $\alpha_i^{(2)}$,

$$\sum_{i=1}^9 \frac{i\alpha_i^{(2)}}{2} \text{Tr} \left[\left(\lambda_i \tilde{m}_e^{(1)} + \tilde{m}_e^{(1)\dagger} \lambda_i \right) \lambda_k \right] = \text{Tr} \left[\left(i s_a t_{2\beta} \mathcal{M} - \tilde{m}_e^{(1)} + \tilde{m}_e^{(1)\dagger} \right) \lambda_k \right], \quad (90)$$

where $\tilde{m}_e^{(1)} \equiv U^{(1)} \tilde{I} m_e = U^{(1)} \tilde{m}_e^{(0)}$. This allows us to solve for the $\alpha_i^{(2)}$ and to exponentiate the corresponding sum to determine $U^{(2)}$.

We continue in this manner, linearizing $U^{(m)}$ at the m th step in order to determine the coefficients $\alpha_i^{(m)}$ (while using the exactly unitary versions of the matrices determined in the previous steps) and then “re-unitarizing” at the end to obtain $U^{(m)}$. After several iterations, the coefficients become vanishingly small and we terminate the process, having obtained an approximation to U_e that is unitary and satisfies Eq. (81) to a high degree of accuracy.

We conclude with two comments:

1. The matrix \mathcal{M} that is produced in Step 7 of the iterative process described in Sec. 3.1 is actually only an approximation to the exact expression and may not be exactly Hermitian. In practice, therefore, we replace \mathcal{M} by $\frac{1}{2}(\mathcal{M} + \mathcal{M}^\dagger)$ wherever it appears in the expressions in this Appendix.²¹
2. Equations (88) and (90) and the analogous expressions for the subsequent steps in the process guarantee that the $\alpha_i^{(j)}$ will be real if \mathcal{M} is Hermitian and if unique solutions exist. When the $\alpha_i^{(j)}$ are determined numerically they generically include small imaginary parts. We discard these.

²¹Even after coercing \mathcal{M} into a Hermitian form it is not guaranteed that a unitary matrix U_e exists such that Eq. (81) is satisfied. To see that this is the case we only need consider the 1×1 case, in which U_e is a pure phase and \mathcal{M} is a real number. For \mathcal{M} larger than a certain value there is no longer a solution for U_e . Our method implicitly assumes that the expressions produced for \mathcal{M} are sufficiently close to the “true” expression that a solution exists for U_e .

C Angular parametrization of $SO(3, \mathbb{C})$

In this appendix, we show that almost all 3×3 complex orthogonal matrices of determinant 1 can be realized as

$$\begin{pmatrix} c_{\eta_1} c_{\eta_3} - c_{\eta_2} s_{\eta_1} s_{\eta_3} & s_{\eta_1} s_{\eta_2} & c_{\eta_1} s_{\eta_3} + c_{\eta_2} c_{\eta_3} s_{\eta_1} \\ s_{\eta_2} s_{\eta_3} & c_{\eta_2} & -c_{\eta_3} s_{\eta_2} \\ -c_{\eta_3} s_{\eta_1} - c_{\eta_1} c_{\eta_2} s_{\eta_3} & c_{\eta_1} s_{\eta_2} & c_{\eta_1} c_{\eta_2} c_{\eta_3} - s_{\eta_1} s_{\eta_3} \end{pmatrix},$$

where $s_{\eta_i} = \sin(\eta_i)$ and $c_{\eta_i} = \cos(\eta_i)$, for suitable choices of complex angles $\eta_i \in \mathbb{C}$. This generalizes the well-known parametrization of $SO(3, \mathbb{R})$ using Euler angles (see for example Ref. [38]).

We start with a lemma that we will need later.

Lemma 2. *Suppose $v^2 + w^2 = 1$ for complex numbers v, w . Then there exists a complex angle η such that $v = \cos \eta$, $w = \sin \eta$.*

Note that $(v + iw)(v - iw) = 1$, so $v + iw \neq 0$. Find any complex angle η such that $v + iw = e^{i\eta}$. This is possible since $v + iw \neq 0$, and the range of e^z is all nonzero complex numbers.

Then $e^{-i\eta} = 1/(v + iw) = v - iw$. Therefore

$$\cos \eta = \frac{e^{i\eta} + e^{-i\eta}}{2} = \frac{2v}{2} = v$$

and

$$\sin \eta = \frac{e^{i\eta} - e^{-i\eta}}{2i} = \frac{2iw}{2i} = w.$$

C.1 Recovering a 3×3 special orthogonal matrix from the middle cross

Proposition 4. *Let*

$$\begin{pmatrix} a & p & x \\ b & q & y \\ c & r & z \end{pmatrix}$$

be an arbitrary element of $SO(3, \mathbb{C})$. Suppose $q^2 \neq 1$. Then

$$\begin{aligned} a &= \frac{-ry - bqp}{1 - q^2}; & x &= \frac{br - qpy}{1 - q^2}; \\ c &= \frac{py - bqr}{1 - q^2}; & z &= \frac{-bp - qry}{1 - q^2}. \end{aligned}$$

If p and r were both equal to 0, then the normalization of the second column would imply $q^2 = 1$, which cannot be. So we may assume $p \neq 0$ (up to symmetry). Likewise, we will assume $y \neq 0$, following a similar argument for the second row.

From the orthogonality of the first two columns, i.e., $ap + bq + cr = 0$, we get

$$ap = -bq - cr, \tag{91}$$

which we may substitute in the normalization condition for the first column, namely $a^2p^2 + b^2p^2 + c^2p^2 = p^2$, to obtain

$$b^2q^2 + c^2r^2 + 2bcqr + b^2p^2 + c^2p^2 = p^2,$$

which is a quadratic equation in c :

$$(1 - q^2)c^2 + (2bqr)c + b^2(q^2 + p^2) - p^2 = 0.$$

The discriminant of this equation is

$$\begin{aligned} 4b^2q^2r^2 - 4(1 - q^2)(b^2(q^2 + p^2) - p^2) &= 4(b^2q^2r^2 - (1 - q^2)(b^2 - b^2r^2 - p^2)) \\ &= 4(-b^2 + b^2r^2 + p^2 + q^2b^2 - q^2p^2) \\ &= 4(b^2(r^2 + q^2 - 1) + p^2(1 - q^2)) \\ &= 4(-b^2p^2 + p^2(1 - q^2)) \\ &= 4(p^2y^2) \\ &= (2py)^2. \end{aligned}$$

Thus

$$c = \frac{-2bqr + \epsilon \cdot 2py}{2(1 - q^2)} = \frac{-bqr + \epsilon py}{1 - q^2}, \quad (92)$$

where ϵ is either 1 or -1 : to be determined.

Since $p \neq 0$, we may divide Eq. (91) by p and substitute Eq. (92) for c to obtain

$$a = \frac{bqr^2 - \epsilon pyr}{p(1 - q^2)} - \frac{bq}{p} = \frac{bqr^2 - \epsilon pyr - bq(p^2 + r^2)}{p(1 - q^2)} = \frac{-\epsilon yr - bqp}{1 - q^2}.$$

In similar fashion, since $y \neq 0$, we obtain

$$x = \frac{-pqy + \epsilon br}{1 - q^2}$$

and

$$z = \frac{-qry - \epsilon bp}{1 - q^2}.$$

By a straightforward calculation, one finds that

$$\det \begin{pmatrix} \frac{-\epsilon yr - bqp}{1 - q^2} & p & \frac{-pqy + \epsilon br}{1 - q^2} \\ b & q & y \\ \frac{-bqr + \epsilon py}{1 - q^2} & r & \frac{-qry - \epsilon bp}{1 - q^2} \end{pmatrix}$$

reduces simply to ϵ . Therefore $\epsilon = 1$ and we are done.

C.2 Complex Euler angles

Theorem 1. *Let*

$$A = \begin{pmatrix} a & p & x \\ b & q & y \\ c & r & z \end{pmatrix}$$

be an element of $SO(3, \mathbb{C})$ such that $q^2 \neq 1$. Then there exist complex angles η_1, η_2, η_3 such that

$$A = \begin{pmatrix} c_{\eta_1} c_{\eta_3} - c_{\eta_2} s_{\eta_1} s_{\eta_3} & s_{\eta_1} s_{\eta_2} & c_{\eta_1} s_{\eta_3} + c_{\eta_2} c_{\eta_3} s_{\eta_1} \\ s_{\eta_2} s_{\eta_3} & c_{\eta_2} & -c_{\eta_3} s_{\eta_2} \\ -c_{\eta_3} s_{\eta_1} - c_{\eta_1} c_{\eta_2} s_{\eta_3} & c_{\eta_1} s_{\eta_2} & c_{\eta_1} c_{\eta_2} c_{\eta_3} - s_{\eta_1} s_{\eta_3} \end{pmatrix}$$

(where $c_{\eta_i} = \cos(\eta_i)$ and $s_{\eta_i} = \sin(\eta_i)$).

Find a complex number u such that $u^2 = 1 - q^2$. By Lemma 2, there is a complex angle η_2 such that $\cos(\eta_2) = q, \sin(\eta_2) = u$. Note that $u \neq 0$; moreover

$$\left(\frac{p}{u}\right)^2 + \left(\frac{r}{u}\right)^2 = \frac{p^2 + r^2}{1 - q^2} = 1,$$

so there exists a complex angle η_1 such that $s_{\eta_1} = p/u$ and $c_{\eta_1} = r/u$. Thus $p = s_{\eta_1} s_{\eta_2}$ and $r = c_{\eta_1} s_{\eta_2}$.

Similarly, there exists a complex angle η_3 such that $b = s_{\eta_2} s_{\eta_3}$ and $-y = c_{\eta_3} s_{\eta_2}$ (here we apply Lemma 2 to the pair $b/u, -y/u$.)

Now we apply Proposition 4:

$$a = \frac{-ry - bqp}{u^2} = \frac{c_{\eta_1} c_{\eta_3} s_{\eta_2}^2 - s_{\eta_3} s_{\eta_1} c_{\eta_2} s_{\eta_2}^2}{s_{\eta_2}^2} = c_{\eta_1} c_{\eta_3} - c_{\eta_2} s_{\eta_1} s_{\eta_3}.$$

Similarly,

$$\begin{aligned} c &= -c_{\eta_3} s_{\eta_1} - c_{\eta_1} c_{\eta_2} s_{\eta_3} \\ x &= c_{\eta_1} s_{\eta_3} + c_{\eta_2} c_{\eta_3} s_{\eta_1} \\ z &= c_{\eta_1} c_{\eta_2} c_{\eta_3} - s_{\eta_1} s_{\eta_3}. \end{aligned}$$

C.3 Other cases

If it happens that $q^2 = 1$ in the above orthogonal matrix A , then there are other ‘‘Euler angles’’ that may be used to parametrize its entries. The easiest way to obtain this is to replace A by $A' = PAQ$ for suitable permutation matrices P and Q , such that the $(2, 2)$ entry of A' is not ± 1 . In other words, even if $q^2 = 1$, there must be some other entry of A that does not square to 1. Permute rows and columns of A until that entry is now in the $(2, 2)$ position, and then apply Theorem 1.

References

- [1] SUPER-KAMIOKANDE collaboration, *Evidence for oscillation of atmospheric neutrinos*, [*Phys. Rev. Lett.* **81** \(1998\) 1562 \[hep-ex/9807003\]](#).
- [2] P. Minkowski, $\mu \rightarrow e\gamma$ at a Rate of One Out of 10^9 Muon Decays?, [*Phys. Lett. B* **67** \(1977\) 421](#).
- [3] R. N. Mohapatra and G. Senjanovic, *Neutrino Mass and Spontaneous Parity Nonconservation*, [*Phys. Rev. Lett.* **44** \(1980\) 912](#).

- [4] T. Yanagida, *Horizontal gauge symmetry and masses of neutrinos*, in *Proceedings: Workshop on the Unified Theories and the Baryon Number in the Universe: Tsukuba, Japan, February 13-14, 1979*, O. Sawada and A. Sugamoto, eds., (Tsukuba, Japan), Natl.Lab.High Energy Phys., 1979.
- [5] S. L. Glashow, *The future of elementary particle physics*, in *Proceedings: Quarks and Leptons, Cargèse, 1979*, Maurice Lévy *et al.*, ed., (NY), Plenum, 1980.
- [6] G. Senjanovic and V. Tello, *Disentangling the seesaw mechanism in the minimal left-right symmetric model*, *Phys. Rev. D* **100** (2019) 115031 [[1812.03790](#)].
- [7] PARTICLE DATA GROUP collaboration, *Review of Particle Physics*, *PTEP* **2022** (2022) 083C01.
- [8] D. Falcone, *Inverting the seesaw formula*, *Phys. Rev. D* **68** (2003) 033002 [[hep-ph/0305229](#)].
- [9] E. K. Akhmedov and M. Frigerio, *Duality in Left-Right Symmetric Seesaw Mechanism*, *Phys. Rev. Lett.* **96** (2006) 061802 [[hep-ph/0509299](#)].
- [10] P. Hosteins, S. Lavignac and C. A. Savoy, *Quark-Lepton Unification and Eight-Fold Ambiguity in the Left-Right Symmetric Seesaw Mechanism*, *Nucl. Phys. B* **755** (2006) 137 [[hep-ph/0606078](#)].
- [11] E. K. Akhmedov and M. Frigerio, *Interplay of type I and type II seesaw contributions to neutrino mass*, *JHEP* **01** (2007) 043 [[hep-ph/0609046](#)].
- [12] J. A. Casas and A. Ibarra, *Oscillating neutrinos and $\mu \rightarrow e, \gamma$* , *Nucl. Phys. B* **618** (2001) 171 [[hep-ph/0103065](#)].
- [13] A. de Gouvea, W.-C. Huang and S. Shalgar, *Parameterizing Majorana Neutrino Couplings in the Higgs Sector*, *Phys. Rev. D* **84** (2011) 035011 [[1007.3664](#)].
- [14] J. C. Pati and A. Salam, *Lepton Number as the Fourth Color*, *Phys. Rev. D* **10** (1974) 275.
- [15] R. N. Mohapatra and J. C. Pati, “Natural” Left-Right Symmetry, *Phys. Rev. D* **11** (1975) 2558.
- [16] G. Senjanovic and R. N. Mohapatra, *Exact Left-Right Symmetry and Spontaneous Violation of Parity*, *Phys. Rev. D* **12** (1975) 1502.
- [17] G. Senjanovic, *Spontaneous Breakdown of Parity in a Class of Gauge Theories*, *Nucl. Phys. B* **153** (1979) 334.
- [18] M. Nemevsek, G. Senjanovic and V. Tello, *Connecting Dirac and Majorana Neutrino Mass Matrices in the Minimal Left-Right Symmetric Model*, *Phys. Rev. Lett.* **110** (2013) 151802 [[1211.2837](#)].
- [19] G. Senjanović and V. Tello, *Probing Seesaw with Parity Restoration*, *Phys. Rev. Lett.* **119** (2017) 201803 [[1612.05503](#)].
- [20] G. Senjanovic and V. Tello, *Parity and the origin of neutrino mass*, *Int. J. Mod. Phys. A* **35** (2020) 2050053 [[1912.13060](#)].
- [21] W.-Y. Keung and G. Senjanović, *Majorana neutrinos and the production of the right-handed charged gauge boson*, *Phys. Rev. Lett.* **50** (1983) 1427.

- [22] S. P. Das, F. F. Deppisch, O. Kittel and J. W. F. Valle, *Heavy Neutrinos and Lepton Flavour Violation in Left-Right Symmetric Models at the LHC*, *Phys. Rev. D* **86** (2012) 055006 [[1206.0256](#)].
- [23] J. A. Aguilar-Saavedra and F. R. Joaquim, *Measuring heavy neutrino couplings at the LHC*, *Phys. Rev. D* **86** (2012) 073005 [[1207.4193](#)].
- [24] J. C. Vasquez, *Right-handed lepton mixings at the LHC*, *JHEP* **05** (2016) 176 [[1411.5824](#)].
- [25] J. Gluza, T. Jelinski and R. Szafron, *Lepton number violation and ‘Diracness’ of massive neutrinos composed of Majorana states*, *Phys. Rev. D* **93** (2016) 113017 [[1604.01388](#)].
- [26] P. S. B. Dev, D. Kim and R. N. Mohapatra, *Disambiguating Seesaw Models using Invariant Mass Variables at Hadron Colliders*, *JHEP* **01** (2016) 118 [[1510.04328](#)].
- [27] A. Das, P. S. B. Dev and R. N. Mohapatra, *Same Sign versus Opposite Sign Dileptons as a Probe of Low Scale Seesaw Mechanisms*, *Phys. Rev. D* **97** (2018) 015018 [[1709.06553](#)].
- [28] K. Kiers, M. Assis, D. Simons, A. A. Petrov and A. Soni, *Neutrinos in a left-right model with a horizontal symmetry*, *Phys. Rev. D* **73** (2006) 033009 [[hep-ph/0510274](#)].
- [29] K. Kiers, J. Kolb, J. Lee, A. Soni and G.-H. Wu, *Ubiquitous CP violation in a top inspired left-right model*, *Phys. Rev. D* **66** (2002) 095002 [[hep-ph/0205082](#)].
- [30] N. G. Deshpande, J. F. Gunion, B. Kayser and F. I. Olness, *Left-right-symmetric electroweak models with triplet Higgs field*, *Phys. Rev. D* **44** (1991) 837.
- [31] B. Kayser, *Neutrino Mass, Mixing, and Flavor Change*, in *Neutrino mass*, G. Altarelli and K. Winter, eds., pp. 1–24, Springer Berlin, Heidelberg, (11, 2003), [hep-ph/0211134](#).
- [32] P. Langacker and S. U. Sankar, *Bounds on the Mass of $W(R)$ and the $W(L)$ - $W(R)$ Mixing Angle ξ in General $SU(2)$ - $L \times SU(2)$ - $R \times U(1)$ Models*, *Phys. Rev. D* **40** (1989) 1569.
- [33] F. R. Gantmacher, *The theory of matrices. Vol. 2*, Translated by K. A. Hirsch. Chelsea Publishing Co., New York, 1960.
- [34] I. Esteban, M. C. Gonzalez-Garcia, A. Hernandez-Cabezudo, M. Maltoni and T. Schwetz, *Global analysis of three-flavour neutrino oscillations: synergies and tensions in the determination of θ_{23} , δ_{CP} , and the mass ordering*, *JHEP* **01** (2019) 106 [[1811.05487](#)].
- [35] M. J. Dolinski, A. W. P. Poon and W. Rodejohann, *Neutrinoless Double-Beta Decay: Status and Prospects*, *Ann. Rev. Nucl. Part. Sci.* **69** (2019) 219 [[1902.04097](#)].
- [36] J. E. Dennis Jr., D. M. Gay and R. E. Welsch, *An adaptive nonlinear least-squares algorithm*, *ACM Trans. on Math. Software* **7** (1981) 348–368.
- [37] S. Gravel and V. Elser, *Divide and concur: A general approach to constraint satisfaction*, *Phys. Rev. E* **78** (2008) 036706.
- [38] L. C. Biedenharn and J. D. Louck, *Angular Momentum in Quantum Physics*. Addison–Wesley, Reading, MA, 1981.